VILNIUS UNIVERSITY

Agnė
KALNAITYTĖ

The photostability and phototoxicity studies of hydrophilic quantum dots in model biosystems

SUMMARY OF DOCTORAL DISSERTATION

Nature sciences,
Biophysics N 011

This dissertation was written between 2014 and 2018 in Vilnius University Life Sciences Center Institute of Biosciences.

Academic supervisor – Prof. Dr. Saulius Bagdonas (Vilnius University, Nature Sciences, Biophysics, N 011).

This doctoral dissertation will be defended in a public meeting of the Dissertation Defence Panel:

Chairman – **Prof. Dr. Daumantas Matulis** (Vilnius University, Nature Sciences, Biophysics, N 011).

Members:

Prof. Dr. Aidas Alaburda (Vilnius University, Nature Sciences, Biophysics, N 011);

Dr. Asta Juzėnienė (The Department of Radiation Biology, Institute for Cancer Research Oslo University Hospital, Nature Sciences, Biophysics, N 011);

Dr. Dalia Kaškelytė (Vilnius University, Nature Sciences, Physics, N 002);

Prof. Dr. Valdas Šablinskas (Vilnius University, Nature Sciences, Physics, N 002).

The dissertation shall be defended at a public meeting of the Dissertation Defence Panel at 1 p.m. on 11 October 2019 in room R-101 of the Life Sciences Center (Vilnius University).

Address: Sauletekio ave. 7, Room No., Vilnius, Lithuania
Tel. +3705 223 4420, +3705 223 4419; e-mail: info@gmc.vu.lt

The text of this dissertation can be accessed at the library of Vilnius University, as well as on the website of Vilnius University:
www.vu.lt/lt/naujienos/ivykiu-kalendorius

VILNIAUS UNIVERSITETAS

Agnė
KALNAITYTĖ

Hidrofilinių kvantinių taškų fotostabilumo ir fototoksiškumo tyrimai modelinėse biosistemose

DAKTARO DISERTACIJOS SANTRAUKA

Gamtos mokslai,
Biofizika N 011

VILNIUS 2019

CONTENTS

Abbreviations

A – optical density;
AC – algae cells;
AF – autofluorescence;
AF int – autofluorescence intensity;
a. u. – arbitrary units;
BA – barrier filter;
BSA – bovine serum albumin;
Chls – chlorophylls;
DM – dichroic mirror;
DW – distilled water;
EX – excitation;
FDW – mineral fertilisers dissolved in distilled water (model ionic solution);
FL – fluorescence;
FWHM – full width at half maximum;
LED – light emitting diode;
PL – photoluminescence;
PL int – photoluminescence intensity;
MPA – mercaptopropionic acid;
MSA – mercaptosuccinic acid;
NPs – nanoparticles;
QDs – quantum dots;
QY – quantum yield;
o. d. u. – optical density units;
PBS – phosphate buffer solution;
PSI –the first photosystem;
PSII – the second photosystem;
ROS – reactive oxygen species;
TGA – thioglycolic acid;
UV – ultraviolet radiation.

1. INTRODUCTION

The rapid development of nanotechnology encouraged the appearance of many new materials and products with novel and unusual properties. Some of these materials and products are up for direct contact with a living organism, and therefore are adapted to interact with an aqueous biological environment. For instance, the biologically compatible nanoparticles (NPs) are usable in cosmetology and medicine: for diagnostics of various diseases, imaging of altered tissues during operations, and treatment of diseases using nanoparticles for drug delivery. However, only some types of nanoparticles have a unique optical property to luminesce when being excited by light irradiation. Photoluminescent semiconductor NPs - quantum dots (QDs), - are used in optical instruments or in monitoring techniques, because QDs can be easily detected and tracked. Also, the applications of photoluminescent hydrophilic quantum dots in imaging of biological systems and as model objects in intracellular studies are rapidly increasing in number.

Modern biotechnological techniques are used to synthesize many different types of quantum dots, varying in parameters such as size, shape, charge, composition, structure, surface coating, etc., all of which influence the interaction of QDs with biosystems. Before QDs are applied in the biological environment, hydrophilic ligands (often having a thiol or amino group) are attached to the surface of heavy metal containing nanocrystals. These ligands make semiconductor nanoparticles water-soluble and facilitate the cellular uptake of them [1], but reduce the stability of QDs optical properties in comparison with hydrophobic ligands. Due to the sensitivity of the spectral properties of hydrophilic semiconductor nanoparticles to environmental factors (medium pH, presence of ions or proteins, other parameters of living systems), quantum dots can also be used as indicators of environmental conditions. On the other hand,

photoluminescence (FL) quenching that occurs in the surrounding environment, when quantum dots are exposed to continuous irradiation, remains a problem using them as luminescent markers. While the physicochemical properties of hydrophilic quantum dots can be influenced by illumination conditions, the changes of QDs photoluminescence induced by absorbed irradiation become extremely important, considering the potential fate of NPs in the biological environment, the threat of QDs toxicity and influences of environmental conditions on these processes. There is still a lack of information about the effects of light on hydrophilic quantum dots, which would help to explain the nature and mechanisms of these effects, to find solutions improving QDs photostability in biological environments, and to encourage the new applications of semiconductor NPs.

The increasing applicability of hydrophilic nanoparticles for everyday use also increases the possibility of accidental release of QDs into the natural waters. In the world's oceans the majority of photoautotrophs, responsible for producing most of atmospheric oxygen, are unicellular algae – an important primary link in the food chain. Chlorophylls in algae cells absorb the energy of the incident light and use most of it for the photosynthesis process, during which cells absorb greenhouse effect stimulating CO_2 gas and reduce its emission into the atmosphere. Some of absorbed and unused energy in the algae cells is emitted via the fluorescence pathway, thus protecting the cell from the harmful effects of light [2]. The ability of protection from excess energy is important for the vital properties of microalgae and for the efficient mechanism of photosynthesis. Like multicellular algae, easily cultivable unicellular algae are rich in nutrients, which are scarce in terrestrial organisms, so they are used in the food industry and in pharmaceuticals. However, algae cells can accumulate various pollutants, such as heavy metals, and wherefore, are often used as model organisms for studying more complex plants and assessing the toxic effects of substances on ecosystems and

8

global processes. The lack of knowledge on the interaction of various hydrophilic semiconductor nanoparticles with microalgae makes it difficult to assess the potential damage caused by the uncontrolled release of NPs into natural waters.

The fluorescence of chlorophylls or autofluorescence (AF) of algae cells can be used for relatively easy spectroscopic monitoring of changes in photosynthetic pigments, thus after being exposed to cellular toxicities as well. The measurements of chlorophyll a fluorescence are used as a rapid, non-intrusive and universal technique that reveals information about the physiological state and processes of protective responses that occur during the life cycle of algae [3]. On the other hand, the spectral shifts and changes in intensity of the photoluminescence of quantum dots can signify that nanoparticles are exposed to environmental conditions (solvent, light) and can become unstable releasing substances that are toxic to living organisms. Thus, spectroscopic and microscopic methods are usable not only for determining the photostability of the QDs, but also studying the impact of nanoparticles on autofluorescence of microalgae.

Since hydrophilic quantum dots are intended for use in biological environments, in this thesis, the stability and photostability of optical properties of hydrophilic CdTe quantum dots capped with thiol ligands were investigated in different ionic media and in medium with bovine serum albumin. The effect of different thiol ligands on the photostability of the spectral properties of quantum dots with ZnS shell was also evaluated in aqueous media and in the presence of serum albumin. In addition to the photostability of CdTe quantum dots capped with mercaptosuccinic acid (MSA) that was assessed in media with wild-type unicellular freshwater *Scenedesmus sp.* and *Chlorella sp.* algae cells, the changes of algae autofluorescence induced by quantum dots were investigated using spectroscopic and microscopic methods, and the effect of nanoparticles on photoadaptive response of algae cells was observed.

The aim of the study and objectives

The aim:

To investigate the photostability of hydrophilic quantum dots (QDs) in model biosystems at different environmental conditions as well as the phototoxic effects of these nanoparticles on unicellular freshwater algae.

Objectives:

1) To investigate the effect of light exposure on spectral properties of CdTe quantum dots capped with mercaptosuccinic acid (MSA) and to estimate dependence of spectral changes on irradiation dose.

2) To evaluate the effects of ionic medium and serum albumin on stability and photostability of optical properties of thiol-capped CdTe and CdSe/ZnS quantum dots.

3) To compare the influence of thioglycolic and mercaptopropionic acids ligands on stability and photostability of spectral properties of CdSe/ZnS quantum dots in aqueous buffer solution in the presence of serum albumin.

4) To investigate the influence of green freshwater unicellular *Scenedesmus sp.* algae on stability and photostability of spectral properties of hydrophilic CdTe-MSA quantum dots in model ionic medium.

5) Using spectroscopy and microscopy methods to investigate the changes that hydrophilic CdTe-MSA quantum dots induced in autofluorescence of unicellular *Scenedesmus sp.* algae and to evaluate the effect of quantum dots on photoadaptation response of algae.

Defended statements

1) The photobleaching of CdTe quantum dots capped with mercaptosuccinic acid (MSA) in aqueous media depends on irradiation dose and can be related to recorded changes in intensity and shape of photoluminescence and absorption spectra.

2) The effects of serum albumin and light on the optical properties of hydrophilic quantum dots depend on both the quality of the capping ligand layer and the composition of the ionic medium.

3) Unicellular algae partially stabilize the spectral properties of CdTe-MSA quantum dots in the presence of environmental factors that reduce QDs stability, such as the ionic medium and applied irradiation.

4) CdTe-MSA quantum dots affect the intensity and spectral shape of autofluorescence of unicellular algae cells, and have negative influence on their photoadaptive responses.

Scientific novelty and actuality

In this thesis several dose-dependent stages of quantum dots photomodification were determined. For the first time there has been shown that these stages are reflected in various spectroscopic parameters: in shape of PL intensity decrease curve and in alterations of the peak PL intensity recovering in dark, in shape changes of absorption and photoluminescence spectra, and in changing kinetics of PL lifetime. These stages of photomodification were combined into a general scheme of the light-induced effects on quantum dots in aqueous medium.

For the first time, it is shown how the dependence of the stability of QDs optical properties on the irradiation dose is affected by ionic medium. It has been shown, how serum albumin and unicellular algae protect quantum dots from the destructive effects of irradiation. It has been revealed that these external factors primarily affect the surface of a quantum dot, so the final effect on the QDs stability and the induced changes of optical properties is more dependent on the response of the capping ligands layer than on that of the shell of the quantum dots.

The nature of observed dependence of spectral changes on irradiation dose for quantum dots interacting with ions, promote the possibility of using quantum dots as ionic biosensors, for example, in the assessment of water pollution.

Also, for the first time, photoluminescence of quantum dots was observed on membranes of algae cells by fluorescence microscopy. The ability of some algae cells to accumulate a part of the quantum dots on cellular membrane, and not to be damaged, opens up the possibilities for the future use of algae cells to gather the quantum dots when nanoparticles get into natural waters.

As nanotechnology is the rapidly developing area, many studies are being done on nanomaterials. However, due to the diversity of nanoparticles and their dependence on environmental conditions, in the scientific literature there is lots of provided conflicting information about the influence of external factors on the properties of quantum dots. The results presented in this thesis about the photostability and phototoxicity of hydrophilic quantum dots in model biosystems will promote the interpretation of the mechanism of general irradiation and medium-induced effects on optical properties of nanoparticles in the light of the findings of various studies, and will help not only to apply nanoparticles more effectively, but also to protect the bioenvironment from the harmful effects occurring under certain conditions.

2. MATERIALS AND METHODS

2.1. Materials

The stability and photostability of spectral properties of quantum dots were measured in phosphate KH_2PO_4 –NaOH buffer solution (PBS) (0.05 M, pH 7), in spring water (pH 7.7) – *Žalia giria* (UAB "Gelsva", no. 31099, Lithuania) and in model ionic medium (FDW, pH 6.2). Model medium was prepared by dissolving mineral fertilisers (Schultz All Purpose Water Soluble Plant Food 20-20-20, Schultz Company, USA) in distilled water to a concentration 160 mg/ml, which was recommended by the manufacturer for indoor plants. In this medium microalgae were grown, too. The initial stock solution of Bovine serum albumin – BSA (Albumin, V fraction, M = 69000 g/mol, Carl Roth GmbH, Germany) was prepared by dissolving BSA powder in small volume of distilled water (DW) until 10^{-3} M, and the final samples with quantum dots (in PBS or FDW) were prepared later (final concentration of BSA – 10^{-5} M). Between the measurements the samples with BSA were kept in the dark at +4 °C.

Quantum dots

Measurements were performed on aqueous suspensions of CdTe quantum dots (550 nm (QD550) and 570 nm (QD570), PlasmaChem GmbH, Germany) that were capped with a mercaptosuccinic acid (MSA) (Fig. 2.1.1) and in aqueous solutions got a negative surface charge. A stock solution of quantum dots (QDs) (2 mg/ml or 3 mg/ml) has been made by suspending powder in distilled water. The initial measurements of the spectra of the QDs samples were made in a 10×4mm quartz cuvette (Hellma, Germany) one hour after the beginning of experiments. The samples of QDs for each experiment were prepared by diluting a stock solution with distilled water, PBS, spring water or model ionic medium to a main final concentration of

25 µg/ml (other concentrations were 100 µg/ml and 200 µg/ml). The QDs samples with microalgae were prepared by pouring a small amount of initial stock solution of quantum dots into FVD medium with algae cells (AC), and keeping the same concentrations of QDs and AC as in the control samples.
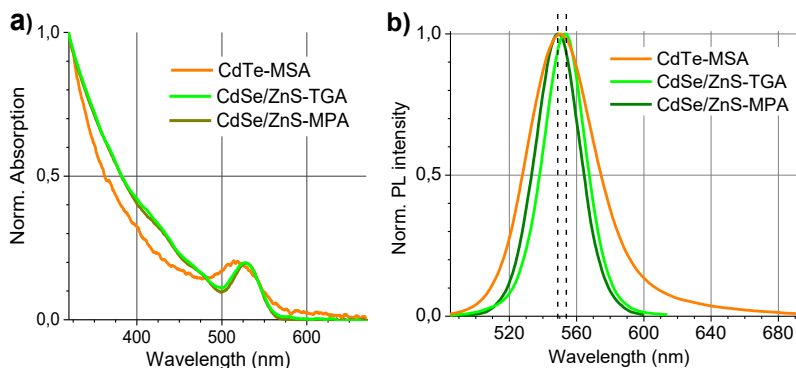

Fig. 2.1.1. Normalised absorption (a) and photoluminescence (b) spectra of quantum dots (core and core/shell, with different surface ligands) in pH 7 phosphate buffer solution.

The CdSe/ZnS quantum dots (Invitrogen, USA) (Fig. 2.1.1), the surface of which had been modified with thioglycolic (TGA) or mercaptopropionic acids (MPA) (PlasmaChem GmbH, Germany) in the Biomedical Physics Laboratory, National Cancer Institute, to make them water-soluble, were studied too. The final concentration of QDs in samples was obtained by dissolving QDs in PBS, and was $3.6 \cdot 10^{-7}$ M.

The unicellular microalgae

The green freshwater unicellular microalgae were isolated from the River Neris near Vilnius city in Lithuania. The dominant species was *Scenedesmus sp*. with some green unicellular *Chlorella sp.* microalgae present in the samples. Algae cells were grown in 10 ml round clear glass vials (Sigma-Aldrich GmbH, Germany) under natural illumination avoiding direct sunlight at room temperature

(20-22°C) with gentle shaking occasionally for almost four months before experiments. Microalgae were grown in model ionic medium. The samples of algae cells were prepared by diluting an appropriate volume of algae culture with FDW medium and then adding a small volume of a stock solution of QDs or distilled water to get the chosen concentrations of both QDs and algae cells.

The samples with microalgae were transferred in 24-well plate (Buddeberg GmbH, Germany) by diluting about 2 ml volume of FDW solution containing algae cells per well with a small amount of the initial QDs stock solution or distilled water. The initial concentration of algae cells in prepared samples was about $2.6 \cdot 10^7$ cells/ml as being counted by means of the Fast-Read 102 plastic counting chamber (Biosigma, Italy). The samples were shaken by hand once per two days to avoid sticking of algae cells.

2.2. Devices

Light sources

The continuous-wave semiconductor laser (532 nm) (Altechna Co. Ltd., Lithuania) was used to irradiate the QDs samples in PBS with albumin. The volume of each sample was 2 ml and the QDs samples were exposed to the laser light in a 10×4 mm quartz cuvette (Hellma, Germany). The spectral measurements were performed immediately after the light exposure, and the samples were kept in the dark at +4 °C between the measurements. The 11.4 J/cm^2 irradiation dose was delivered during five minutes.

The violet light emitting diode (LED) (404 ± 9 nm (FWHM), 30 mW/cm^2 at a distance of 8 cm) was used to expose the QDs samples, too. The 2 ml of each sample were poured in a 24-well plate (Buddeberg GmbH, Germany) and the collimated light was directed from the bottom of a plate to illuminate an area of 1 cm^2 in selected wells, at the same time covering other samples with a protective screen made from aluminium foil or keeping them in another plate.

Before the registration of the QDs spectra, the samples were stirred every time and transferred from the wells to a quartz cuvette, if needed.

A part of experiments, especially with algae, were done on the samples keeping them between the measurements under controlled illumination conditions. The plate was constantly illuminated during 12 hours using a white fluorescent lamp (11W/827, Osram Duluxstar, China) from a distance of about 25 cm at room temperature. A 12/12 h "light/dark" cycle was applied, and the samples of algae cells were preadapted to these illumination conditions starting at four days before the main experiment (a group I).

Spectrometers

The initial absorbance spectra were measured immediately after the surface modification of CdSe/ZnS quantum dots using a Varian Cary Win UV absorption spectrometer (Varian Inc., Australia). Samples were measured in a 10×4 mm quartz cuvette. The initial photoluminescence spectra were measured with a Varian Cary Eclipse spectrofluorimeter (Varian Inc., Australia). An excitation wavelength for photoluminescence was set at 405 nm, the excitation and emission slits were 5 nm. For the rest of experiments with samples in a cuvette, an AvaSpec-3648 fibre optic spectrometer (Avantes, Netherlands) was used to register absorption spectra, and a LS55 spectrofluorimeter (PerkinElmer, USA) was used to register PL and PL excitation spectra. An excitation wavelength for PL of CdSe/ZnS quantum dots was set at 450 nm, the excitation slit was 4 nm, and the emission slit was 3 nm. For the rest of experiments with QDs and algae samples the excitation wavelengths were set at 405 nm, 411 nm, 440 nm, 450 nm, 460 nm and 480 nm, the excitation and emission slits were 3 nm.

The optical fibre system (OFS) was used to register the photoluminescence of QDs and autofluorescence of algae spectra in plates. A tip of a bifurcated fibre-bundle made of seven 200 μm

fibres (Somta Ltd, Latvia) was used to excite and collect the fluorescence signal of samples from the bottom of a well. One arm with the central fibre in it was attached to a low intensity (< 1 mW) excitation light source emitting at 405 nm (Ocean Optics, USA), while the six encircling fibres were used to collect the fluorescence signal into another arm. To cut off excitation light, it was attached to a filter holder containing a 510 nm yellow long-pass emission filter, which was connected to the spectrometer USB2000 (Ocean Optics, USA) using a single 400 μm fibre.

QDs PL lifetime measurements were carried out with a spectrophotometer FL920 (Edinburgh Instruments, UK). The excitation source was the picosecond pulsed diode laser EPL-405. For analysis of kinetics data the FAST (Edinburgh Instruments, UK) and OriginPro8 (OriginLab, USA) software were used.

Microscopes

The microscopy measurements were done by means of a fluorescence microscope *Nikon eclipse 80i* through the 40x/0.75 *Plan Fluor DIC M/N2* objective (Nikon). The pictures were captured with a colour *Nikon Digital Sight DS-SMc* camera (Nikon, Japan) using three different excitation / emission cubes with following optical properties: **UV-2A** (a excitation range $\Delta\lambda_{ex}$ = 330-380 nm, a dichroic mirror (DM) 400 nm, a barrier filter (BA) > 420 nm), **V-2A** ($\Delta\lambda_{ex}$ = 380-420 nm, DM 430nm, BA > 450nm) and **G-2A** ($\Delta\lambda_{ex}$ = 510-560 nm, DM 575 nm, BA > 590 nm).

Some of measurements were done using a fluorescence microscope *Nikon eclipse TE 2000–U* with a confocal scanning Cl si system (Nikon, Japan) using a x60/1.4 *Plan Apo VC oil* objective. The pictures were captured with a DFC-290 RGB CCD (Leica, Germany) camera. During these microscopic measurements the fluorescence was excited with a diode laser, λ_{ex} = 405 nm. For fluorescence images the three-channel RGB detector was used, which had a set of band-pass filters: 433-467 nm (blue channel), 500-

590 nm (green channel) and 620-755 nm (red channel). The pseudo colours were set in images depending on the region of band-pass filters: the luminescence of QDs was seen in green channel, the blue autofluorescence of algae – in blue channel, and red AF – in red channel. Image processing was done using the „Nikon EZ-C1 Bronze version 3.80" software.

2.3. Methods

The volume of each sample was 2 ml. All initial spectroscopic measurements were done an hour after the samples preparation. The QDs samples were kept at different conditions between the measurements:
  - in the dark at +4 °C (in a study with protein);
  - in the dark at room temperature (in one study with DW);
  - in the shadow at room temperature (covered with protective screen made from aluminium foil);
  - in a room lit by natural daylight, avoiding direct sunlight (in study with QDs and algae cells (a group II));
  - at room temperature under 12/12 h "light/dark" cycle illumination conditions (in a study with algae cells (a group I)).

The dose-dependent photobleaching of quantum dots
The final concentration of each sample of CdTe-MSA quantum dots (QD550 and QD570) in distilled water was 25 μg/ml, and in FDW - 25 μg/ml, 100 μg/ml and 200 μg/ml. The triplets of each sample have been measured to obtain all mean spectra of experiments with QDs samples in DW and in FDW introduced in 3.2 and 3.3 chapters, respectively. The samples then were kept in the dark at +4 °C for a day until the beginning of irradiation experiments as well as for one additional hour after irradiation with a single dose of 27 J/cm^2. The spectral measurements were performed immediately after exposing 2 ml of a solution in a 24-well plate to a LED light to

obtain the cumulative dose (Fig. 3.1.2). The 3.6 J/cm^2 irradiation dose were got during two minutes irradiating.
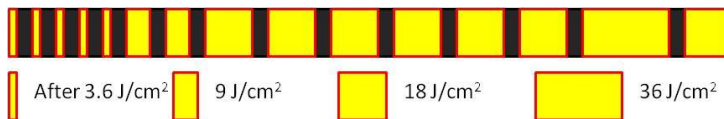

Fig. 2.1.2. The schema for accumulation of irradiation doses.

In between exposures, the solution of each QDs samples was stirred, and the PL spectra were measured with an optical fibre system at five randomly chosen spots in a well within five minutes (Fig. 2.1.3). The spectroscopic measurements of samples before exposure, after 27 J/cm^2 and 108 J/cm^2 irradiation doses were made in a quartz cuvette, too.

Fig. 2.1.3. The option scheme of spots in a well, where measurements of the algae AF intensities and quantum dots PL were done.

The additional (lasting 15-30 minutes) measurements of the changes in PL intensity of QD570 at 567 nm (corresponding to the peak position of a PL band) were performed in the dark on a randomly chosen single spot immediately after exposing samples with 3.6 J/cm^2, 7.2 J/cm^2, 27 J/cm^2 and 108 J/cm^2 doses of irradiation.

The interaction between CdTe-MSA quantum dots and algae cells (3.6 chapter)

To study the spectral properties of quantum dots and their interaction with algae cells under prolonged incubation (18 days), three types of samples were prepared, containing QDs in FDW, algae cells and QDs in FDW with algae cells. At the beginning, volumes of about 2 ml from a sample containing algae cells (a group I) in FDW

were prepared in two sextets and then poured into a 24-well plate. Then six wells of the samples containing microalgae and other six wells filled with FDW were supplemented with 25 μl of a QDs stock solution (2 mg/ml) to get the final concentration of QDs (25 μg/ml), thus marking the beginning of the experiment, during which the 12/12 illumination cycle was maintained for 18 days without changes. The spectral measurements on the samples were performed with OFS one hour after incubation and were continued on the subsequent days at the beginning of the "light" part of the cycle from the bottom of the well at five randomly chosen spots. The samples were gently stirred every time before starting the PL intensity measurements.

The effect of CdTe-MSA quantum dots on algae cells (3.7 chapter)

To avoid the redundant exposure of QDs, during the experiment the samples with microalgae were kept in a room lit by natural daylight, avoiding direct sunlight (a group II) and the growing conditions were not changed after preparation of the samples. To determine the effect of QDs on autofluorescence properties of algae cells under natural ambient illumination, the two types of samples with algae cells were prepared in doublets: the control samples and the samples with QDs, to which small volumes (65 μl) of the QDs stock solution (3 mg/ml) were added to get a final QDs concentration of 100 μg/ml. The volumes of 2 ml of each sample were poured in a 12-well plate (Buddeberg GmbH, Germany). The samples remaining in the dark overnight (about 12 hours) were used to measure the slow part of the photoinduced changes in the fluorescence of chlorophylls (Kautsky effect). The additional measurements of AF intensities at 683 nm, the peak of the main fluorescence band, were registered with an optical fibre system from the plate bottom and lasted about 20 min. The doublets of each sample were also used for measurements in a cuvette to obtain the mean autofluorescence spectrum.

<u>The fluorescence quantum yield</u>

Quantum yield (QY) of the PL of quantum dots was calculated using the equation given in a work by Eaton [4]. The solution of rhodamine B (Sigma-Aldrich, Germany) (c = 4.7× 10^{-6} M) in 64 % w/w aqueous ethanol was used as the PL standard and the fluorescence quantum yield of rhodamine B Φ_s =0.7 was used. The values of refractive indexes of water (n=1.34 [5]) and 64 % ethanol solution (n_s = 1.36 [6]) at 20°C were included in QY calculations. The errors of PL QY of QDs were evaluated taking into account the systematic errors of absorption measurements (± 0.001 o. d. u.).

3. RESULTS AND DISCUSSION

3.1. The stability of optical properties of CdTe-MSA quantum dots in different ionic solutions

The stability study of optical properties of CdTe (QD550) quantum dots (25 μg/ml) capped with mercaptosuccinic acid in aqueous solutions with different ionic compositions revealed influence of ions on structural stability of quantum dots. The last (excitonic) band at 520 nm in an absorption spectrum of quantum dots was the narrowest and had the highest relative intensity being measured in a QDs sample with distilled water (DW) (Fig. 3.1.1). The excitonic absorption band of the QDs samples in pH 7 phosphate buffer solution (PBS) was slightly broader than in DW, and this band in distilled water with dissolved fertilisers – a model ionic solution (FDW) – was shifted about 3 nm to the long-wave side of the spectrum.

Although the optical density of the QDs samples in the spring water (SW) increased in the blue spectral region, the relative intensity of the excitonic band became lower and a shift of its peak toward the long-wave region was the largest among all samples with ionic media. Also, the PL intensity in the QDs sample with SW was the lowest, and the shift of a band (about 20 nm in comparison with

DW) to the red side of spectrum was the largest (Fig. 3.1.2). The initial PL intensity of the CdTe-MSA quantum dots in both PBS and model ionic medium (FDW) was about 3.5-times lower than in pure distilled water (Fig. 3.1.2 a).
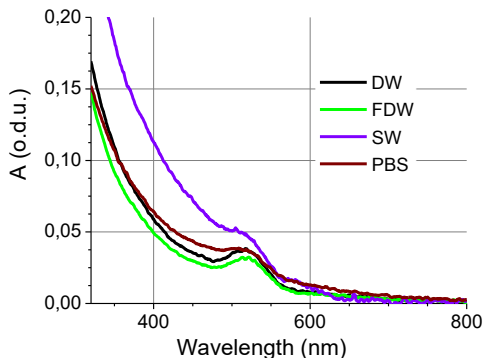

Fig. 3.1.1. The initial absorption spectra of CdTe-MSA quantum dots (25 μg/ml) in different ionic solutions. DW- in distilled water, FDW – in model ionic medium, SW – in spring water, PBS – in a phosphate buffer solution.

The mean values of the PL quantum yield of the quantum dots were $21.8 \pm 0.8\%$ in phosphate buffer solution, $23.5 \pm 0.5\%$ in the model ionic medium, while about three times bigger value was obtained in distilled water ($67.3 \pm 1.4\%$). The peak of PL band of quantum dots was recorded at 547 nm in distilled water, in the ionic medium the PL band it was shifted about 2 nm and a shift in PBS was about 5 nm to the long-wave side of spectrum (Fig. 3.1.2 b). The decrease of the PL intensity of the quantum dots (Fig. 3.1.2 a) as well as the shift of the excitonic absorption band (Fig. 3.1.1) and the PL band to a red spectral side being recorded on the first day after sample preparation in ionic solutions (Fig. 3.1.2), could be explained by formation of aggregates [7, 8].
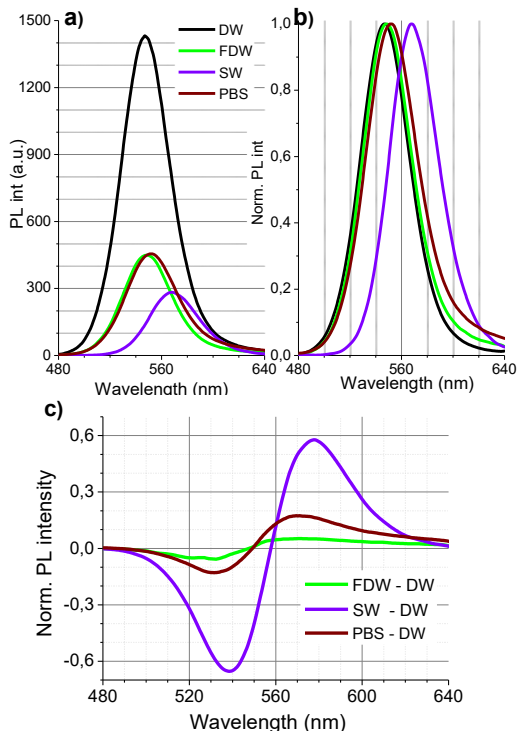
Fig. 3.1.2. The initial photoluminescence spectra of CdTe-MSA quantum dots (25 μg/ml) in different ionic solutions (a) (normalised at peak value (b)) and the normalised differential spectra (c) of PL intensity of QDs, which reflect the relative spectral differences between the PL intensity of QDs in ionic media and those in distilled water. $\lambda_{ex} = 405$ nm.

One of the reasons for the formation of QDs aggregates in aqueous media is the higher ionic strength of the solution [7, 9] resulted by cations of multivalent metals [10]. Therefore, the interaction between multivalent cations, anions, or their hydrated forms in ionic media, and the surface ligands of negatively charged CdTe quantum dots have a stronger effect on the initial PL spectra of NPs (Figs. 3.1.1 and 3.1.2). In addition, the formation of ionic

23

complexes with surface ligands of QDs eventually can locally influence the distribution and density of ligands.

An asymmetric increase in PL intensity on the red part of the PL spectrum (or "a tail") (Fig. 3.1.3 b) was observed in QDs samples in ionic media and this "tail" was higher in PBS than in FDW solution. The interaction of ions with the surface of the NP likely can also stimulate detachment of ligands, while uncovered structural defects on core surface of the quantum dot being exposed to dissolved ions in the medium may cause a decrease in PL intensity and other spectral changes (Figs. 3.1.2 and 3.1.3). The presence of ions near ligands on defective surface regions of the core creates an important precondition for lowering the energy levels of quantum dots [11, 12], which is likely to stimulate the appearance and increase of a "tail" in the red part of the PL spectrum (Fig. 3.1.3).

The absorption and PL spectra of the initial QDs samples show that the best and the most stable spectral parameters (the highest PL intensity and QY, the narrowest spectral band, etc.) are in distilled water compared to other ionic media. Therefore, to study the effect of ionic medium on the PL spectra, normalised initial spectrum recorded in distilled water was subtracted from the corresponding normalised PL spectra (Fig. 3.1.3 c).
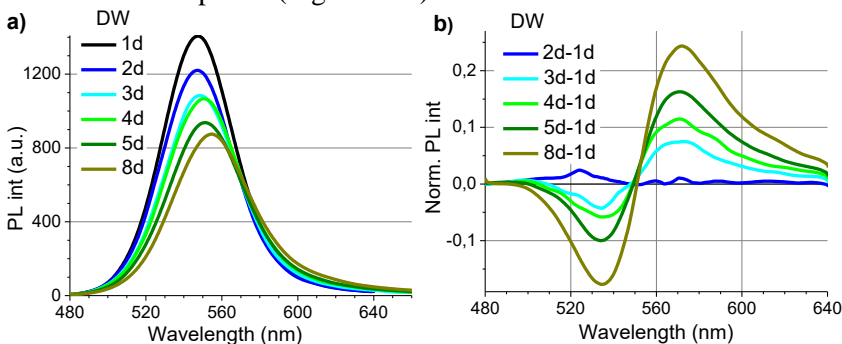
Fig. 3.1.3. The photoluminescence intensity of CdTe-MSA quantum dot samples (25 mg/ml) stored in dark, at room temperature and recorded at different days (a), and the normalised differential spectra (c) of PL, which

reflect the relative spectral differences occurring during time QDs samples in distilled water. $\lambda_{ex} = 405$ nm.

The optical density of the QDs coated with MSA remained unchanged in distilled water after one week in the dark at room temperature, but the PL intensity decreased and was only about two-thirds of the initial value on 8th day (Fig. 3.1.4 a). A shift of the PL band to the long-wave side of a spectrum was also observed together with the formation of a "tail" on a red part of the PL spectrum, which was recorded in FDW and PBS media immediately after sample preparation (Figs 3.1.4 a and 3.1.4 b). It is likely that these temporal changes in DW samples are caused by the small amount of ions, which still are in DW, and can eventually affect the spectral PL properties of quantum dots in the same way as ions dissolved in ionic media.

3.2. The changes in photostability of CdTe-MSA quantum dots: dependence on irradiation dose

When using quantum dots as luminescent markers, it is important to evaluate the influence of environmental factors, including irradiation, on the stability of QDs photoluminescence, therefore the changes in related spectral properties of quantum dots have been measured after different irradiation doses. The decrease pattern of the PL intensity being observed at peak position (Fig. 3.2.1 a) in QD570 samples prepared in DW was uneven and depended on a delivered dose: it started with a relatively steep initial decline, then temporarily flattened and got steeper again at the end.

The changes in values of the peak PL intensity, which were measured after four certain irradiation doses of QD570 and then normalized to an initial value before exposure, are reported in Fig. 3.2.1, b. The PL intensity started to increase in the dark after delivering the first dose of 3.6 J/cm^2 and reached a steady state in about 20 minutes, but the initial intensity had not been fully restored.
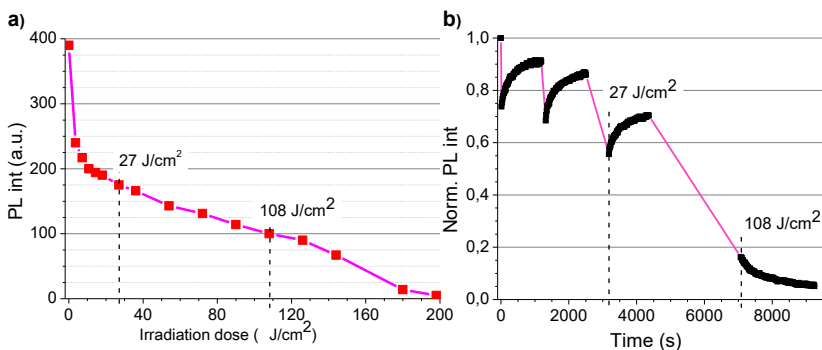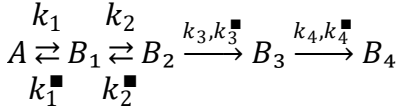
Fig. 3.2.1. The decrease of the photoluminescence intensity of CdTe-MSA quantum dots (QD570) (25 mg/ml) measured at the maximum of a PL band immediately after exposures with LED radiation (a) and the changes of the normalized PL intensity measured at 567 nm immediately after exposing samples with 3.6 J/cm^2, 7.2 J/cm^2, 27 J/cm^2 and 108 J/cm^2 doses of irradiation (b). The photoluminescence of QDs was registered by means of an OFS (λ_{ex} = 405 nm).

The changes in values of the peak PL intensity, which were measured after four certain irradiation doses of QD570 and then normalized to an initial value before exposure, are reported in Fig. 3.2.1, b. The PL intensity started to increase in the dark after delivering the first dose of 3.6 J/cm^2 and reached a steady state in about 20 minutes, but the initial intensity had not been fully restored. A similar pattern was also observed during the same period after higher doses (7.2 and 27 J/cm^2), only the extent of recovery was reduced in the latter case. The faster process contributed more in fitted data (by applying an exponential function with two time coefficients) after a 7.2 J/cm^2 dose, but the fitting of the data recorded after delivering 27 J/cm^2 dose showed an increased contribution of a slower process at the expense of a faster one. It seems that, during the recovery period of quantum dots photoluminescence in the dark, several interchanging and overlapping processes occur. In contrast to the observed rise, the PL

intensity of QDs was decreasing in the dark after the exposure with 108 J/cm^2 dose.

The observed changes in PL intensity allowed assuming a tentative sequence of processes occurring during exposure of quantum dots and afterwards:

$$\begin{array}{cc} k_1 & k_2 \\ A \rightleftarrows B_1 \rightleftarrows B_2 \xrightarrow{k_3, k_3^{\blacksquare}} B_3 \xrightarrow{k_4, k_4^{\blacksquare}} B_4 \\ k_1^{\blacksquare} & k_2^{\blacksquare} \end{array}$$

where A marks unexposed quantum dots, B_i – certain states of photoproducts, while k_i and $k_i^{\blacksquare}$ are the time coefficients for light-induced processes and those occurring in the dark. The absence of total recovery of photoluminescence intensity after initial exposure as well as the two-exponential nature of the process imply the light-induced transformation of QDs (A) into several concomitant products (B_1 and B_2), which can undergo reverse changes in the dark with corresponding rate coefficients.

The ability to recover lost PL intensity after exposure was reported for QDs with a shell and was attributed to a reversion of some photoinduced lattice defects, storing samples after irradiation in the dark [13]. Those defects, which didn't annihilate and became permanent, could eventually result in a complete quenching of the luminescence [14]. The higher doses of exposure seem to cause a shift in a chain of processes that accelerate damage formation on the NPs surface in different media stimulating more changes, which can further proceed in the dark in a self-sustaining way and lead to formation of irreversible states (B_3 and B_4). The gradual photomodification of the CdTe-MSA quantum dots, which changed the pattern of PL intensity variation recorded in the dark immediately after the irradiation, also found its reflection in the corresponding changes of the absorption and the photoluminescence spectra. While the PL intensity of exposed QDs decreased sharply after the smallest doses, the absorbance of QD550 was unaffected even after a single

exposure to 27 J/cm^2 (Fig. 3.2.2 a). However, such dose reduced the peak PL intensity of QDs by three-fifths of the value being measured before irradiation and caused a slight broadening of the PL band (Fig. 3.2.2 b). After a total exposure to 108 J/cm^2 the intensity of excitonic absorption band at about 520 nm had almost vanished (Fig. 3.2.2 a), the PL intensity decreased about 20 times, and the PL band of exposed QDs shifted about 9 nm to a red spectral side in comparison with unexposed QDs (Fig. 3.2.2 b).
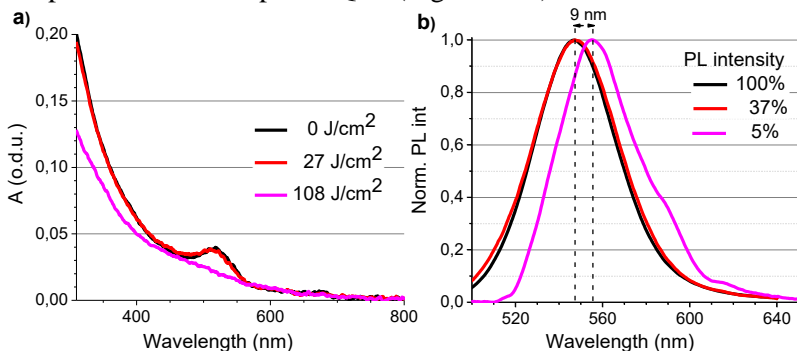

Fig. 3.2.2. The absorption (a) and the PL (b) spectra of CdTe-MSA quantum dots (QD550) (25 mg/ml) in distilled water at a second day of experiment: before irradiation and after exposure to two different doses. λ_{ex} = 405 nm.

The decay kinetics of excited states photoluminescence that were registered in solutions of unexposed QD570 and after exposing the samples to 18 J/cm^2 and 72 J/cm^2 (Fig. 3.2.3), yielded the average decay lifetimes $< \tau >$, which were calculated using a formula provided in [15]. The increased value of the average decay lifetime of PL excited states $< \tau >$ after a lower dose of irradiation ($< \tau > = 30$ ns) in comparison with unexposed QDs ($< \tau > = 27$ ns) and its later decrease after a higher dose ($< \tau > = 13$ ns) reflected the presence of dose-dependent stages in the changing PL properties. An increase in the average PL lifetime $< \tau >$ after a lower irradiation dose defines

28

processes that are considered to originate from the surface-related photoluminescence of the CdTe quantum dots [16].
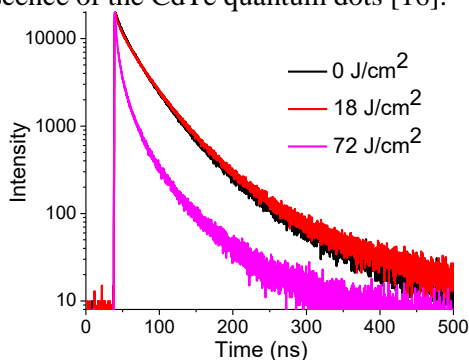

Fig. 3.2.3. The photoluminescence decay kinetics recorded for unexposed CdTe-MSA quantum dots (QD570) (25 mg/ml), and after exposing samples to the doses of 18 J / cm^2 and 72 J / cm^2. $\lambda_{ex} = 405$ nm.

Although detachment of ligands and their redistribution on the surface of the QDs core are attributed to processes occurring under dynamic equilibrium, ligands interacting with water and dissolved ions could be eventually washed out from QDs surface. That kind of ligands detachment has been considered as a displacement reaction causing formation of QDs aggregates, which increase in size as the process progresses [17]. It has been noted that ligand with a relatively short chain can bring the surface of a nanoparticle and water molecules in close proximity and affect the photostability of the QDs [18]. The luminescence quenching under irradiation was ascribed to the formation of defects due to the detachment of ligand molecules from QDs and spontaneous aggregation [19, 20].

According to the obtained results, the absorption spectrum was still unaffected in QD550 samples exposed with 27 J/cm^2 dose (Fig. 3.2.2 a), which was apparently too low dose to induce the significant detachment of surface ligands. However, the highest dose of irradiation might have had an impact on most of ligands, leading to enhanced aggregation probability, which was reflected in the

strongly suppressed intensity of both excitonic absorption (Fig. 3.2.2 a) and the PL bands, the bathochromic shift of the PL (Fig. 3.2.2 b), and decreased value of the average decay lifetime of PL excited states (Fig. 3.2.3). It seems that any external factor affecting the integrity of a surface coating can stimulate the aggregation; however, process occurring under dark conditions has a much longer time scale than that induced by exposure to the light [21].

One might assume that the irradiation further disturbed a bonding interaction of ligands with a QDs core, possibly resulting in partial ligand detachment and facilitating the contacts with the surrounding water molecules, which can adsorb to the surface of the quantum dots and passivate surface traps during illumination [22, 23]. The spectroscopic changes that took place in the dark might reflect a partial restoration of the photodamage caused to the surface of QDs after exposure of the samples to low doses of irradiation. Thus, certain transitive transformations in the photomodification process of QDs might be linked to the particular features appearing in normalized differential PL spectra as well as to different stages of the PL intensity decrease, which are seen in figures 3.2.1 and 3.2.4.
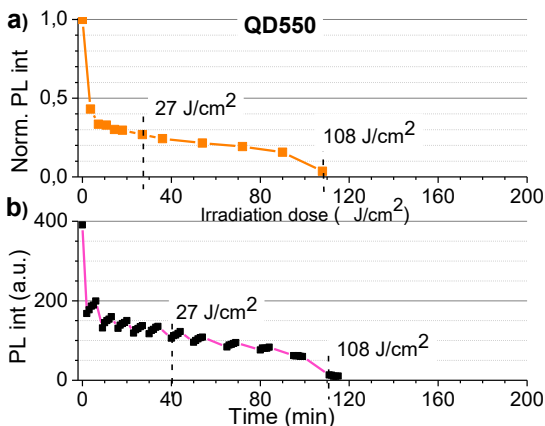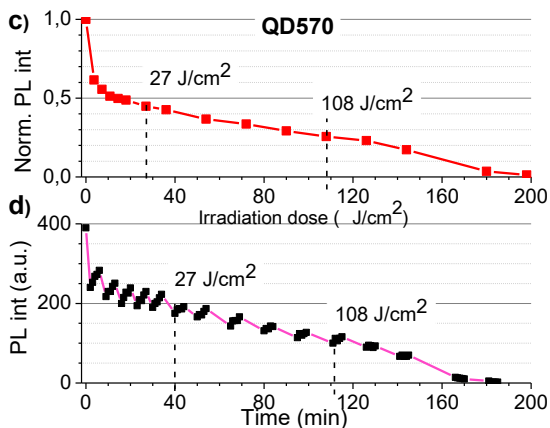
Fig. 3.2.4. The decrease of the normalized photoluminescence intensity of CdTe-MSA quantum dots QD550 (a, b) and QD570 (c, d) (25 mg/ml) measured at the corresponding maximum of a PL band immediately after exposure of samples (a, c), and the changes in the PL intensity of QDs shown in a scale of the real experiment time (b and d). The photoluminescence of QDs was registered by means of an OFS (an excitation wavelength − 405 nm.

Figure 3.2.4 shows the photoinduced changes of the PL intensity at the peak positions for QD550 and QD570, and both QDs demonstrated the dependence of the PL intensity decrease on a delivered dose in a similar way revealing three stages of photobleaching. Fitting of the experimental data being registered until moderate 72 J/cm^2 and 126 J/cm^2 doses of irradiation (Figs. 3.2.4 a and 3.2.4 c) with an exponential function has revealed that a biexponential decrease pattern gave the closest resemblance to the PL intensity, yielding similar t_1 time coefficient for both QDs. The slower decrease of the PL intensity (described by a bigger value of a fitted time coefficient) was relatively more manifested in the case of QD570, which initially possessed a smaller QY of photoluminescence.

Owing to an observed dose-dependent effect of applied exposures on photoluminescence properties of CdTe-MSA quantum dots, the three stages might be distinguished in the pattern of the photoinduced decrease of the PL intensity. While the transitions between these stages of PL decline were not sharp, nevertheless, each stage can be associated with the corresponding alterations of the peak PL intensity being measured at the periods of dark between exposures. Interesting that the QD550 had stopped recovering the PL intensity in the dark after the moderate dose of about $72 - 90$ J/cm^2, while QD570 needed a higher dose - about 126 J/cm^2 (Figs. 3.2.4 b and 3.2.4 d), that is, at about the same corresponding doses that marked the final acceleration of PL intensity decrease for those QD.
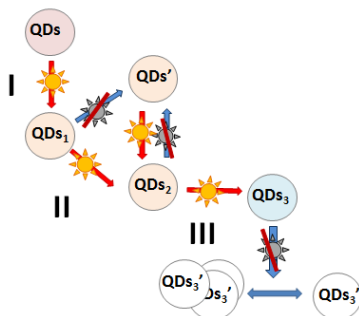
Fig. 3.2.5. Schematic picture of the light-induced processes being reflected in the pattern of the PL intensity changes of exposed CdTe-MSA quantum dots in distilled water.

Thus, the comparative analysis of the photoinduced gradual changes in absorbance and photoluminescence features of CdTe-MSA quantum dots in DW allowed distinguishing three universal stages of the photomodification, as depicted in a suggested schema of processes (Fig. 3.2.5).

The first stage of QDs photomodification occurred after initial exposure, during which a rapidly decreasing PL intensity of QDs indicated the suppressed PL quantum yield. The structure of a ligand molecule might in fact affect its capacity to cap tightly the surfaces

with different curvature depending on the size of a QDs core. Moreover, a high PL quantum yield implies an orderly arrangement of capping molecules. It might be that the initial irradiation resulted in the rearrangement of ligands on the surface of a nanocrystal and a partial breakage of some coordination bonds, implying that the first stage depends on the size of QDs and the integrity of the initial ligands surface layer. The second stage of the QDs photomodification involves transitive processes, which were reflected in as yet unaffected excitonic absorption band (Fig. 3.2.2 a), slight broadening of a PL band (Fig. 3.2.2 b) as well as in a slower decrease of the PL intensity and recovery of the reduced PL intensity in the dark between irradiation (Fig. 3.2.4). The explanations concerning the photoenhancement of the PL intensity of freshly synthesized QDs noted the importance of the surrounding solvent, the likely reason for that in the case of aqueous medium being the adsorption of water molecules on the defective sites at the surface of the exposed QDs, which led to increased QY of PL [22, 23]. The core-ligand interaction is more photodisturbed after higher exposure doses, when some completely broken coordination bonds can be changed by molecules from media, which had been attracted to the QDs core. The third stage of photomodification is characterized by the biggest and irreversible changes in optical properties of QDs. During this stage the photoinduced decrease of PL intensity was again accelerated, while the PL stopped restoring and continued to decrease in the dark (Fig. 3.2.4), the intensity of excitonic band at 520 nm (Fig. 3.2.2 a) and the PL became reduced almost completely as well as the PL band shifted to the red spectral side (Fig. 3.2.2 b), and the values of average decay lifetime of PL excited states decreased (Fig. 3.2.3). The exposure with higher doses probably induced such interaction between ligands and water that might have facilitated the complete breakage of some MSA molecules, thus opening the direct access to the QDs core surface for the solvent, which can enhance the formation probability for irreversible

superficial core defects leading to the irreversible changes of the spectral QDs properties. As it has been noted, the irradiation of MPA-capped QDs for short periods caused, mainly, surface changes, and prolonged irradiation with a mercury lamp light induced degradation of the QDs [18]. It seems that the disintegration of a protective MSA capping layer on the QDs surface during the final stage might be a reason of induced aggregation.

3.3. The photostability of CdTe-MSA quantum dots in ionic solutions

Since molecules of surrounding media could affect light-induced changes in the spectral properties of CdTe-MSA quantum dots (QD550), even in DW, it was important to evaluate the influence of different ionic media, which had a significant effect on PL stability of quantum dots immediately after preparation of samples, on the photoinduced changes in spectral properties of nanoparticles, too. The intensity of PL in phosphate buffer solution was lower than that recorded in DW (Fig. 3.1.2) and decreased even in the case of a control, unexposed QDs sample, the PL intensity of which nearly halved after the first hour of the experiment (Fig. 3.3.1), while the PL band shifted to the long-wave side of spectrum. Meanwhile, immediately after irradiation with 11.4 J/cm^2 dose the PL intensity of the QDs sample decreased 1.4 times, and this change was greater than that of unexposed QDs over the same period. As in the control sample, the PL intensity of the exposed QDs was still decreasing after irradiation, and after two hours it was only one-fifth of the initial PL value in the irradiated samples and reached about two-fifths of the unexposed QDs.
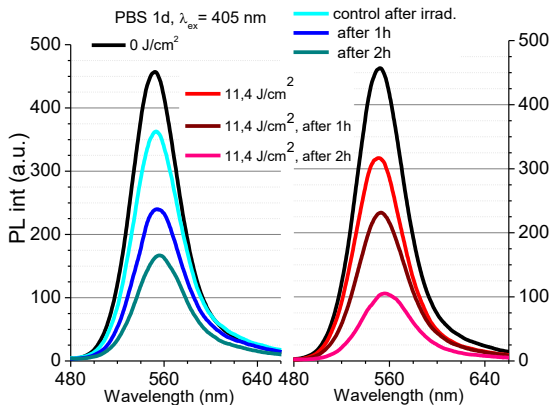
Fig. 3.3.1. The photoluminescence intensity of exposed and control CdTe-MSA quantum dot samples (25 mg/ml) in PBS at the first day of experiment before irradiation and intensity changes immediately after exposure (532 nm radiation), after one and two hours stored in dark. λ_{ex} = 405 nm.

Comparing the relative spectral changes in exposed and controls QDs samples, it can be seen that the light exposure actually suppressed the shift of the PL band to the long-wave spectral side and also reduced the "tail" on its red side. After two hours, the red "tail" in the PL spectrum of exposed samples remained lower than in the control, suggesting that the detachment of molecules, ligands and ions from the core was likely stimulated by the light exciting QDs surface. The redistribution of ligands and ions on the QDs surface during irradiation, when more ligands can detach and more ions can attach to the nanoparticle, subsequently accelerated the QDs aggregation in the case of exposed samples compared to controls.

The PL intensity of CdTe-MSA (QD550) quantum dots in the model ionic medium (FDW) (Fig. 3.3.2) decreased relatively more than in DW after preparation of the samples. The peak intensity of QDs photoluminescence decreased further in both solutions after irradiation (27 J/cm^2): it reached only about two-fifths of its initial

value in DW and about three-fifths - in ionic medium. During an hour after the irradiation the PL intensity partially recovered in the case of the samples prepared in DW, but continued to decrease in FDW. Not only the changes of ions concentration in solution can change the PL intensity, but also the ionic composition of the medium influences the defective states of QDs surface and the non-radiative exciton relaxation [24].
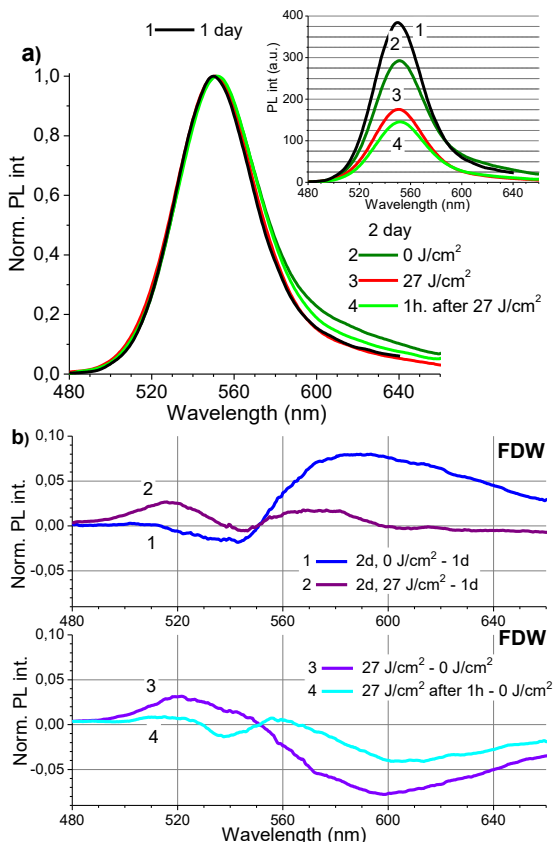

Fig. 3.3.2. The mean PL spectra of CdTe-MSA quantum dots (QD550) samples recorded (a) in model ionic solution before and after a single exposure to irradiation dose of 27 J/cm^2 at 404 nm as well as after subsequent storage in the dark for 1 h. The differential spectra (b) of PL

intensity of QDs reflecting: (top) time-induced changes and (bottom) light-induced changes that were registered immediately after the exposure and 1 h later. $\lambda_{ex} = 405$ nm

The irradiation dose of 27 J/cm^2 applied to the sample in FDW caused a symmetrical increase in PL intensity in both sides of the difference spectrum as well as a decrease of the PL "tail", returning its relative intensity to the initial value (Fig. 3.3.2 b, curve 2). This temporary spectral redistribution of the PL possibly due to adsorption of different ions from medium on the surface of the QDs core that were replaced with solvent molecules, for example, water, the adsorption of which can also assist in the passivation of surface defects [22, 23]. Although the PL intensity of QDs in DW slightly recovered in the dark after irradiation, it continued to decrease in ionic media (Figs. 3.3.1 and 3.3.2 a). The observed decrease in relative intensity of the red "tail" of the PL band was temporary and it was recovering in the dark, and these spectral changes of the QDs PL band in the model ionic solution were similar in nature to the initial medium-induced changes associated with the effects of ions that become associated as they approach the surface of the QDs core. Thus, the light-induced redistribution of ions on the QDs surface was temporary, because the weakened ligand-core interaction during irradiation allowed the ions from the medium to come near the surface of the NP more easily, thereby accelerating the time related medium-induced changes.

Measurements of the spectral properties of irradiated QDs samples in different aqueous media showed that the ionic composition of the medium significantly affects the light-induced changes in the QDs spectra, regardless of whether these changes were light-induced or complex and occurred in combination with the medium-induced effects over time. The ions from the medium approach the QDs core and adsorb to its surface, which induce the growth of the "tail" in the long-wave part of the PL band, and later

37

the ions-induced ligand detachment facilitates QDs aggregation, which is reflected by shifting the PL band to the long-wave side of spectrum. The absorbed radiation that activates the surface of the nanoparticle also creates conditions for the redistribution of all molecules in the neighbourhood, and the extent to which the defects of QDs surface will be exposed after this redistribution as well as whether they will be passivated in the dark depends on the composition of the medium after delivering particular exposure.

The influence of model ionic solutions on the dose-dependent spectral properties and photostability of quantum dots

The relative decrease in PL intensity of CdTe-MSA quantum dots varied depending on the composition of aqueous solutions: for the same QDs concentration (25 µg/ml) it was stronger in FDW than in distilled water. Extrapolation of the data depicted in figure 3.3.3 a implies that about 10 percent of the initial value of QD550 photoluminescence remained after exposure to a dose of 23 J/cm^2 in FDW, while a dose of about 96 J/cm^2 was needed to get the same decrease in DW. When the identical exposure conditions were maintained during the experiments with samples containing higher concentrations of QDs (100 µg/ml and 200 µg/ml) in FDW, the exposures to doses of about 39 J/cm^2 and 60 J/cm^2 were needed in order to reduce the PL intensity to 10 percent of its initial value. In addition, the three stages of photomodification distinguished itself in the pattern of the photoinduced PL decrease for CdTe-MSA quantum dots in distilled water and were also present in the pattern of the PL decrease for QDs in model ionic solution.
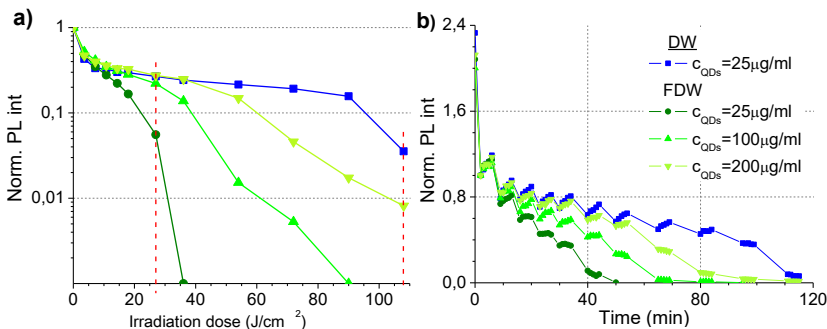
Fig. 3.3.3. The decrease of the normalized PL intensity of CdTe-MSA quantum dots (QD550) in model ionic solutions with three different concentrations of QDs (25, 100 and 200 µg / ml) that was measured at the maximum of a PL band immediately after exposure of the samples (a), and the changes in the normalized PL intensity of QDs shown in a scale of the real experiment time (b). A single concentration of QDs (25 µg / ml) in DW is shown for comparative purposes. The photoluminescence of QDs was registered by means of an OFS (λ_{ex} = 405 nm.).

Comparison of the data (Fig. 3.3.3 b) revealed that after the initial doses of irradiation the normalized PL intensity increased similarly in all solutions of QDs during five subsequent minutes in the darkness. However, the capacity of the PL intensity to increase in the darkness had diminished after repeated exposures, and the PL intensity even started to decrease later on, depending on the QDs concentration and the ionic composition of the sample solutions. Apparently, the increase of resistance to light-induced changes in PL that was observed in the model ionic solution and was characteristic for higher QDs concentrations might be attributed to decreased ion-ligand ratio in the medium. The importance of ions in the medium for the transformations during an intermediate stage of photomodification affecting the integrity of the QDs capping layer is reflected by the revealed dependence of its duration on the QDs concentration and the composition of medium – the stage was shorter in the samples with lower QDs concentration and/or higher amount

39

of ions in the medium, i.e., it was affected with decreasing ratio of QDs to ions.

Thus, the same three dose-dependent stages of QDs photomodification as in DW were observed in the ionic medium, too, and were reflected in the same spectroscopic parameters: in the specific pattern of the decrease curve of PL intensity, in the variations of peak intensity in the dark between irradiations, in the spectral changes of absorption and PL bands. Since the first stage depended only on the initial quality of the capping layer of ligands on the QDs surface, it was almost unaffected by ions in the medium. However, the second stage begins when part of the coordination bonds of ligands are broken and the molecules present in the medium come closer to the surface of the QDs, so its duration apparently depended on the ions present in the medium and shortened in the samples with decreasing ratio of QDs to ions. Thus, when complete detachment of some ligands, such as MSA molecules occurred in the third stage, stimulating the aggregation of quantum dots, it also depended not only on the absorbed irradiation dose, but also on the activity and concentration of the ions in media.

3.4. The effect of protein on stability and photostability of quantum dots in different ionic solutions

To investigate the effect of another factor, the biological environment, on the photostability of QDs, bovine serum albumin (BSA) was added as a model protein to different ionic media with CdTe-MSA quantum dots. Protein molecules significantly affected the PL stability of QDs in ionic media immediately after preparation of samples (Fig. 3.4.1 a), so that the photoluminescence intensity of QDs increased in media with protein, but in model ionic solution still barely reached half the value of the PL intensity measured in DW, and even less of it (two fifths) - in PBS samples.
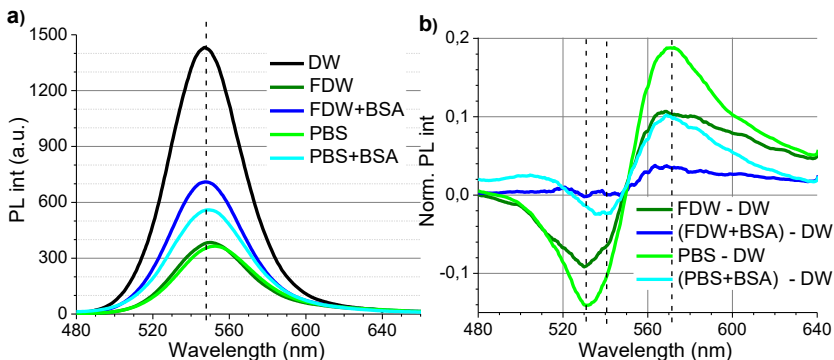
Fig. 3.4.1. The initial photoluminescence spectra of CdTe-MSA quantum dots (25 μg/ml) in different solutions (a) and the normalised differential spectra (b) of PL intensity, which reflect the relative spectral differences between the PL intensity of QDs in different media and those in distilled water. DW- in distilled water, FDW – in model ionic medium, PBS – in phosphate buffer solution, and with serum albumin (BSA) in FDW and PBS media. $\lambda_{ex} = 405$ nm.

The addition of albumin molecules not only induced the increase of PL intensity in QDs samples, but also partially supressed the shift of PL band to long-wave spectral side that occurs in ionic media, i.e. resulted in its shift to short-wave side (Fig. 3.4.1 b) (toward the spectral position of the PL peak in DW). It is likely that the protein might have suppressed the effect of ionic media, which promotes NPs aggregation and is reflected in spectral characteristics like the decrease of PL intensity and the shift of band to the long-wave side of spectrum, by increasing the stability of the QDs ligand layer. It has been shown that proteins can improve the photoluminescent properties of some QDs, probably by forming a protective coating [25 - 27], which not only prevents quantum dots from approaching each other and forming mutual bonds, but also reduces the detaching ability of QDs ligands being stimulated by ions present near the surface of QDs. Besides the aforementioned shift, the forming "tail" in the long-wave part of the PL band was still observed in ionic

41

media. The intensity of this "tail" was lower in the presence of protein in both ionic media, but did not disappear, probably, due to some ions that penetrated to the surface of the QDs through the protein coating.

The PL intensity of QDs in PBS decreased rapidly throughout the experiment, regardless of the presence of protein in the medium (Fig. 3.4.2). The average PL quantum yield of unexposed QDs samples calculated in PBS was 21.8 ± 0.8 %, while QY values increased to 30.0 ± 0.2 % for samples with albumin. Although the PL signal in both solutions almost disappeared after a day, in the medium with protein the PL intensity was three quarters higher, and the calculated QY value was slightly higher, even if it was only 4.0 ± 0.3 %.
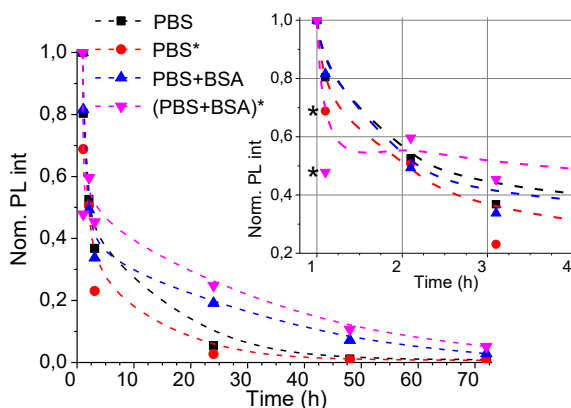
Fig. 3.4.2. The normalised PL intensities of CdTe-MSA quantum dots (25 mg/ml) in PBS (with and without albumin), which were registered at the maximum of the band during three days. Between measurements the samples were stored in the dark, at +4°C temperature. * marks the data of exposed (532 nm laser light, 11.4 J/cm^2 dose) samples that were irradiated immediately after the initial measurements at the first day. $\lambda_{ex} = 405$ nm.

The relative PL intensity of irradiated QDs samples in PBS was lower than that of unexposed QDs after a day or two days. The relative PL intensity decreased more slowly in the irradiated QDs

samples with protein than in the unexposed samples, and this tendency continued during the whole experiment. It is an interesting observation that although the PL intensity in medium with BSA had the largest relative decrease after irradiation, it increased slightly after one hour in the dark (Fig. 3.4.2). It is likely that some damage to the QDs ligand layer caused by the irradiation did not become irreversible due to protein coating formed on NPs, which served as both protective measure from ionic species approaching the QDs surface in the medium and preventive measure from detachment of ligands from the surface of QDs.

The shift of the PL band of quantum dots to the long-wave side of spectrum was slower immediately after samples preparation in the medium with albumin than in the medium without BSA, so a relatively smaller shift also was observed during one hour after irradiation. Protecting the PL intensity by protecting the surface of QDs, protein is likely to delay nanoparticles at an earlier stage of light-induced changes.. This explanation is also supported by the fact that the light-induced changes in medium with BSA were temporary, the PL intensity increased slightly after one hour in the dark, and the spectral changes of PL band shape also approached those observed in the control samples.

The PL intensity of QDs in the model ionic solution decreased to one fifth of the initial value during eight days after preparation, whereas after irradiation with 27 J/cm^2 dose PL decreased immediately and reached these values on the second day of the experiment (Fig. 3.4.3). Although the PL intensity of the quantum dots has increased together with the average PL quantum yield, which increased from $23.5 \pm 0.5\%$ to $41.3 \pm 0.4\%$ in the presence of protein after the samples preparation in FDW medium, the PL intensity in the samples with BSA decreased relatively faster than in the samples without BSA during the first day. The exposure of QDs to a 27 J/cm^2 irradiation dose in FDW medium with albumin resulted in a decrease of relative PL intensity, but similarly as in the case of

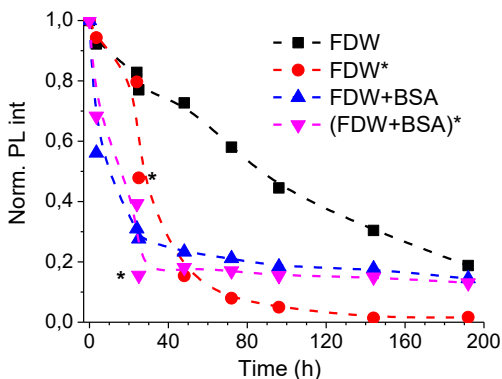QDs samples in PBS with albumin, it recovered slightly after irradiation.

Fig. 3.4.3. The normalised PL intensities of CdTe-MSA quantum dots (25 mg/ml) in model ionic solution (with and without albumin), registered at the maximum of a PL band during 8 days, between measurements samples were kept in dark, at +4°C temperature. * marks the spectra of exposed (404 nm radiation, 27 J/cm^2 dose) samples, irradiated after 24 h after samples preparations. λ_{ex} = 405 nm.

The spectral changes related to the effect of medium ions on QDs stability were less pronounced in samples with protein, and no shift of a PL band was observed. After irradiation, the intensity of "tail" in the long-wave part of QDs photoluminescence band decreased in all samples, where it was recorded, regardless of the initial intensity of the band and the composition of medium (PBS or FDW, and both solutions with BSA). This confirms that the spectral "tail" is caused by ions located near the QDs surface, and that the redistribution of molecules on the NPs surface during irradiation is not limited by the presence of albumin in the medium. Also, regardless of the ionic composition of the medium, a partial recovery of PL intensity was observed in QDs samples with BSA during an hour after irradiation, which indirectly evidences the ability of albumin to slow down the photodamage of the QDs capping layer.

44

Experimental results revealed that the stability of the spectral properties of quantum dots in samples of the same kind and concentration was different in different ionic media, including those with albumin, which also demonstrated different medium-dependent effects. BSA slightly slowed the medium-dependent process in PBS, in which a rapid decrease in PL intensity of QDs was observed immediately after samples preparation. The PL intensity of QDs was more stable in model ionic solution than in PBS, while before irradiation in both samples with protein the PL intensity decreased sharply at first, but later this drop stabilized. Such differences demonstrated different protective activity of the protein with respect to the interaction of ligands and various ions adsorbing on the QDs surface. The spectral properties of QDs are affected more intensively in PBS solution than it happens in FDW, thus the protein is also less effective protecting them from the influence of ions on the integrity of QDs surface. Regardless of the presence of albumin, the spectral changes of QDs samples observed in PBS and FDW media after irradiation were probably not only caused by different activity of ions, but also affected by different doses of irradiation. The changes of QDs PL observed in PBS after an irradiation dose of 11.4 J/cm^2 are more typical to the earlier stage of photomodification than those observed in FDW media after a dose of 27 J/cm^2. However, BSA reduced the shift of the QDs photoluminescence band to long-wave side of spectrum, potentially protecting nanoparticles against the ion-induced damage on the surface and not allowing the ions to accelerate the photomodification process during irradiation. Thus, although the nature of the protein interaction with CdTe-MSA quantum dots do depends on the composition of the ionic medium, serum albumin is able to slow down the ion-induced and irradiation-accelerated processes that negatively affect the integrity of NPs surface and, consequently, the spectral properties of quantum dots in both solutions, PBS and FDW.

3.5. The dependence of quantum dots stability and photostability on surface ligands in phosphate buffer solution

This section reviews experiments on the stability and photostability of spectral properties of CdSe quantum dots with a ZnS shell capped with thioglycolic (TGA) and mercaptopropionic (MPA) acids in phosphate buffer solution, at pH 7. Different ligands allowed to study and compare in more detail their influence on the spectral properties of QDs, their stability and photostability. Although the ZnS shell allowed CdSe nanoparticles to obtain higher values of photoluminescence QY (Fig. 3.5.1) compared to CdTe-MSA quantum dots, the extent of the QY value was strongly dependent on the type of ligand: higher QY values were obtained for QDs modified with MPA ligands (58.3 ± 1.7 %) than for QDs modified with TGA (33.2 ± 0.3 %).
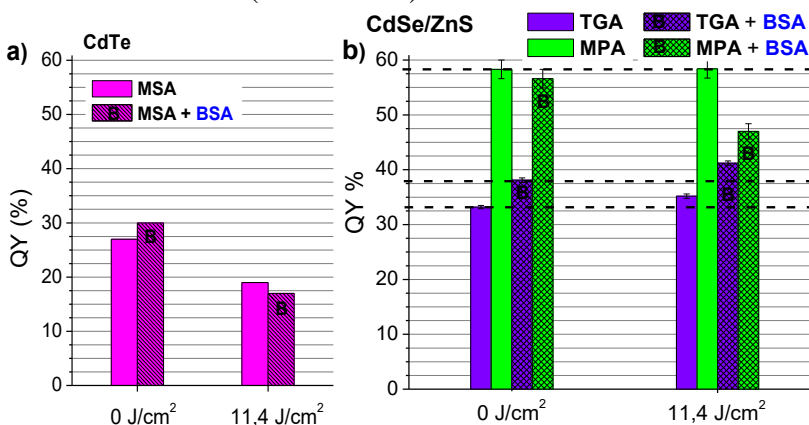

Fig. 3.5.1. The values of quantum yield of CdTe quantum dots capped with MSA ligands (a), and CdSe quantum dots with a ZnS shell and capped with TGA and MPA ligands (b) calculated before exposure of samples and immediately after irradiation with a 532 nm laser (with and without albumin in PBS).

As discussed in previous chapters, the PL QY increased by several percent after the addition of albumin to CdTe-MSA samples in PBS, but decreased again after irradiation (Fig. 3.5.1). The interaction of the CdSe/ZnS quantum dots with the protein and the changes in spectral properties of QDs depended on the type of capping ligand (Fig. 3.5.1 b). The quantum yield of TGA-capped QDs in the solution with protein increased slightly, so the effect was similar to that observed for CdTe-MSA. However, the quantum yield of MPA-capped QDs in the same solution, on the contrary, decreased slightly. Therefore, it is likely that the ability of albumin to form a protective coating on the surface of QDs depends on ligand molecules. After irradiation of the samples with the same dose, the quantum yield of CdSe/ZnS-MPA photoluminescence in the buffer solution did not change, but decreased by about 10 % in the medium with protein. On the other hand, although QDs capped with TGA ligands did not have as high initial QY values as QDs capped with MPA, these values increased after irradiation in both solutions: with and without BSA molecules.
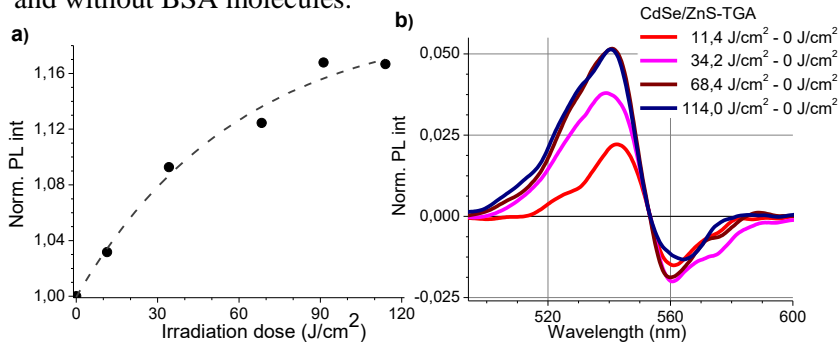

Fig. 3.5.2. The dependence of normalised PL intensities (at 549 nm) of CdSe/ZnS-TGA quantum dots in PBS on irradiation doses (a dotted line marks the results of approximation with an exponential function) (a) and normalised differential spectra being calculated for corresponding irradiation doses (b). $\lambda_{ex} = 450$ nm.

47

The exposure of QDs by light whereby the solvent molecules on the QDs surface cause redistribution of the coating layer molecules in the case of imperfect initial coating, might result in a more orderly structure and improved passivation of surface defects. On the other hand, the PL intensity of quantum dots with a smoother surface layer of ligands and higher QY values at the beginning of experiment is expected to decrease and then be able to recover in the dark.
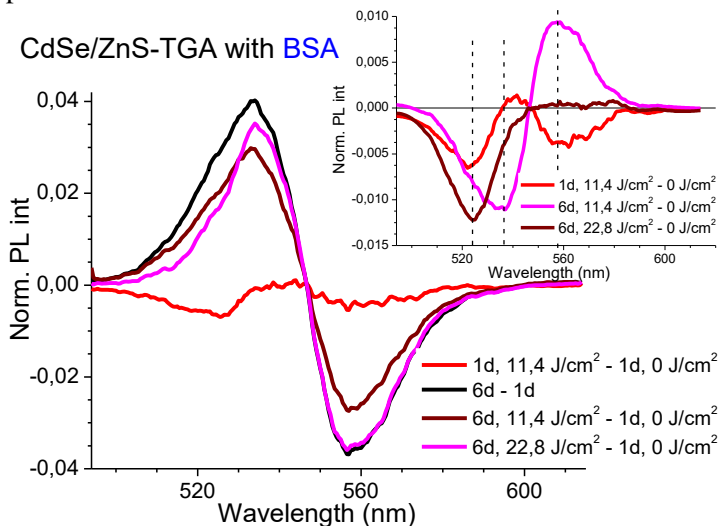
Fig. 3.5.3. The normalised differential spectra of CdSe/ZnS-TGA quantum dots in PBS with albumin, calculated after additional irradiation at different experiment days. $\lambda_{ex} = 450$ nm.

The PL intensity of the CdSe/ZnS-TGA quantum dots increased until about 114 J/cm^2 irradiation dose and reached almost 120% of the initial intensity (Fig. 3.5.2 a). The relative spectral changes in the PL band reflecting its shift to the short-wave spectral side were observed as well when evaluating the increase in the PL intensity of TGA capped QDs samples after irradiation (Fig. 3.5.2 b). As in the case of solutions of QDs without shell, a similar shift of the PL band to long-wave side of the spectrum was observed for core/shell QDs after three days, suggesting that this spectral change is not related to

48

ion-induced alterations in the QDs core, but is due to the effect of ions on the integrity of the coating layer, the damage of which leads to aggregation of QDs. The effect of irradiation with 11.4 J/cm^2 dose was still present after one day, and, as it can be seen by comparing the measured changes, the shift of PL bands to the long-wave side of the spectrum was shorter for the exposed QDs samples than for non-irradiated ones. Similar photoinduced relative spectral changes of the PL band were also observed in samples of QDs without shell in the phosphate buffer solution after a day, only after lower doses of irradiation compared to control samples.

The intensity of PL spectra of TGA capped QDs in phosphate buffer solution with BSA had a time-related tendency to increase, and the band – to move to the short-wave side of the spectrum (Fig. 3.5.3). The realised ability of the protein to form a protective surface layer on the surface of QDs is known to cause a shift in the PL spectrum to the short-wave side of the spectrum [12], and it is likely that the formation of this layer also can improve the photoluminescence properties of certain QDs samples. The PL intensity of the QDs samples with BSA on the first day after irradiation increased further, and the PL band narrowed, probably, due to the increased homogeneity in NPs sizes. After additional exposure to the same dose on the 6th day, the PL intensity of the QDs sample decreased, and the band shifted to the long-wave side of the spectrum. A higher total irradiation dose again increased the PL intensity of the QDs, while the spectral changes in the PL band occurred at different rates: the decrease on the short-wave side of spectrum was slower. Comparing to the latter changes, the spectra of CdTe-MSA quantum dots demonstrated the opposite pattern – the decreasing PL intensity accompanied by a faster band decrease on the short-wave side of the spectrum.

The irradiation of the CdSe/ZnS-MPA quantum dots also induced an increase in their PL intensity, but the change was very temporary, and after few minutes the PL intensity returned to its initial value

(Fig. 3.5.4 a). There was also a temporary shift of the PL band towards the short-wave region that was observed in the differential spectra after the irradiation (Fig. 3.5.4 b). As with TGA capped QDs (Fig. 3.5.2 b), the relative extent of this shift to the short-wave spectral region is associated with an increase or decrease in PL intensity: the increase in PL intensity of the TGA capped QDs was saturated with the increasing shift, whereas in the case of QDs capped with MPA this shift became smaller with the decreasing PL intensity. The light-induced increase in the PL intensity together with the shift of the band to the short-wave side of the spectrum have been explained by QDs surface passivation, which may involve interactions with oxygen or water molecules [28].
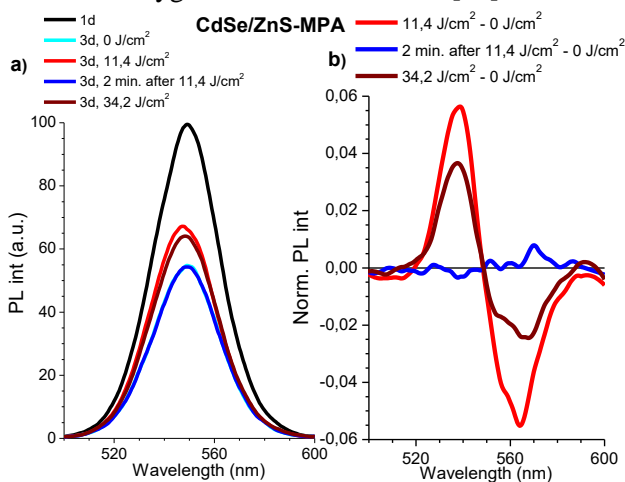
Fig. 3.5.4. The changes in PL intensities of CdSe/ZnS-MPA quantum dots in PBS during three days and after exposure (a), and the normalised differential spectra reflecting light-induced changes in PL. $\lambda_{ex} = 450$ nm.

The PL intensity of the CdSe/ZnS-MPA quantum dots in PBS with protein slightly increased immediately after irradiation, but after a couple of minutes, after mixing the sample, a decrease in intensity, even below its initial value before irradiation, was observed (Fig.

3.5.5.) Similarly to the TGA-capped QDs or the MPA-capped QDs in solutions without protein, the PL band shifted to the short-wave side of the spectrum after irradiation.
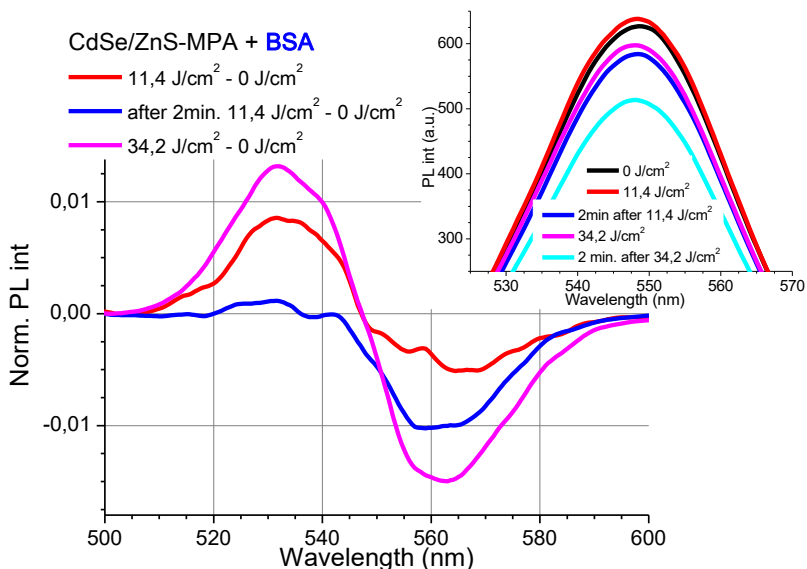
Fig. 3.5.5. The light-induced changes in normalised differential spectra of CdSe/ZnS-MPA quantum dots in PBS with albumin, and the PL intensities measured at the peak value immediately after irradiation and after a couple of minutes of samples stirring. $\lambda_{ex} = 450$ nm.

Thus, due to the ability of the protein present in the medium to form a protective coating on the QDs surface, the presence of serum albumin resulted in an increase in the PL intensity of the CdSe/ZnS QDs and a shift of PL in the short-wave side of the spectrum. Although QDs capped with longer-chain ligands often have higher initial PL quantum yields, these ligands form weaker bonds to the QDs surface [29] making the optical properties of these QDs more sensitive to external factors. Therefore, the interaction of a protein with a QDs surface can be multiple, and its nature also depends on the length of the ligand chain. Serum albumin cannot properly bind

51

to MPA-capped QDs, because the longer chain of the MPA molecule hinders such bonding, and a long-term protective coating of protein on QDs surface does not form. In addition, due to protein- assisted passivation of the QDs surface during irradiation, the PL intensity of CdSe/ZnS quantum dots capped with both the TGA and MPA ligands increased after irradiation, and the band shifted to the short-wave side of the spectrum. Nevertheless, the albumin and the light exposure act as two independent factors affecting the QDs surfaces, and their mutual effects might be suppressive or enhancing on the optical properties of QDs, depending on the structure and quality of the capping layer. The quantum yield of CdSe/ZnS quantum dots capped with TGA increased in medium with BSA, and spectral properties were more stable than in protein-free medium. Irradiation also increased the PL intensity and QY of CdSe/ZnS-TGA quantum dots. However, the PL intensities, the QY, and stability of these properties in CdSe/ZnS-MPA quantum dot samples decreased in the medium with BSA, and irradiation caused just a short-term increase in PL intensity.

3.6. The influence of algae on the stability and photostability of CdTe-MSA quantum dots

Changing environmental conditions strongly affect the surface layer of QDs and may be critical for studying their bioaccumulation and toxicity [30]. To better understand the effect of water-soluble CdTe quantum dots capped with MSA on freshwater green unicellular algae, it is important to evaluate the influence of algae growing media and illumination conditions on the spectral properties of the QDs itself. Although the initial PL intensity of CdTe-MSA quantum dots (QD550) was 3.5 times lower in model ionic solution (FDW) than in DW, the PL intensity of QDs in FDW with algae cells (AC) (*Scenedesmus sp.* and *Chlorella sp.*) was only halved and did not differ significantly from the PL intensity recorded in FDW with serum albumin (Fig. 3.6.1). Since the protein demonstrated

protective activity against ion-induced damage on NP surface by forming an additional protective layer on the QDs surface, it is likely that algae cells were also able to partially protect the surface of quantum dots from detrimental influence of ions.
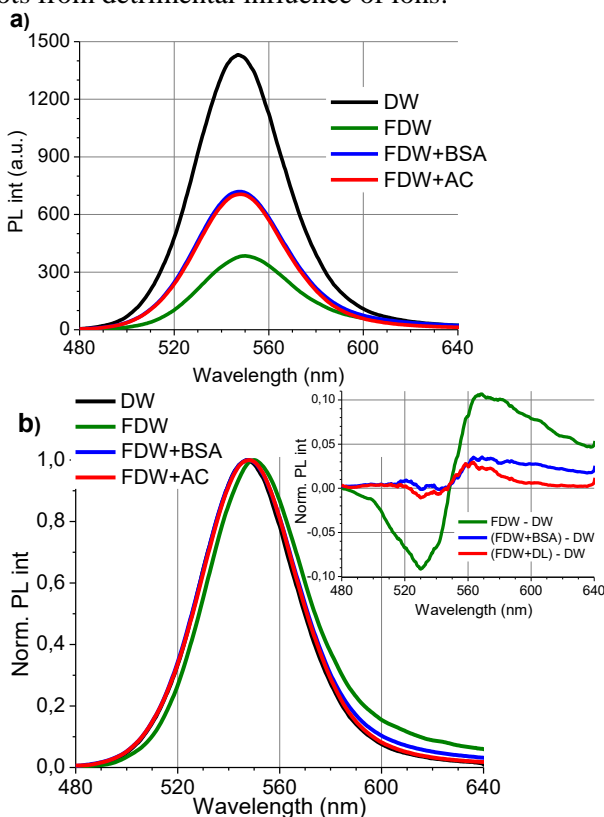
Fig. 3.6.1. The initial PL intensities of CdTe-MSA quantum dots (a) (normalised and differential spectra are shown in (b)) in different media (25 μg/ml): in distilled water (DW), in model ionic medium (FDW) and in FDW with algae cells. $\lambda_{ex} = 405$ nm.

The maximum intensity of the PL band in the QDs samples was registered at 548 nm in distilled water, and while the PL band was shifted about 2 nm to the long-wave side of spectrum in the model

ionic solution, this shift did not occur in solutions with protein or algae cells (Fig. 3.6.1 b). Nevertheless, the time-related medium-dependent effect on the integrity of the capping ligand layer, being reflected by the shift of the PL band to the long-wave side of the spectrum, was observed in QDs samples with AC, only less pronounced in comparison with samples in FDW without AC (Fig. 3.6.1 b). However, the PL band did not have a red "tail" at all, which, although of low intensity, was still recorded in the FDW solution with protein.

These QDs samples were subsequently stored under the same conditions as those used for growing of algae cell - applying "light/dark" (12/12) illumination cycle, so that all samples of quantum dots were continuously exposed to moderate illumination for half a day. It seems that the interaction between QDs core and ligands becomes weaker in the medium with AC during a day (resulting in relatively slower decrease of the PL intensity in the short-wave part of the spectrum), and the time-related NPs aggregation (a shift towards the long-wave side of the spectrum) has occurred after the detachment of some ligands. However, in the medium with unicellular algae, the PL of the QDs samples was more intensive not only immediately after preparation of the samples, but also remained almost unchanged during a day (decreased from 49.2% to 48.7%) (Fig. 3.6.2 a, curves 1 and 2). The stabilizing effect of unicellular algae on the decrease in PL intensity of QDs has been reported in seawater [31], and has been attributed to extracellular products that can modify the chemical structure of QDs surface and modify the properties of QDs [32, 33]. If the changes in optical properties of QDs were the strongest effect being caused by interactions between ions and the capping ligands of QDs, then unicellular algae present in the medium and also their extracellular products [34] could compete with the QDs for dissolved ions.

Another important factor affecting the optical properties of QDs was irradiation. The intensity of the PL band decreased significantly

after additional QDs irradiation in the model ionic solution, the peak of PL band shifted about 7 nm to the short-wave side of the spectrum, toward the initial position (recorded immediately after the sample preparation), and the full width at half maximum (FWHM) of the band increased. Three hours after irradiation the shift to the short-wave side of the spectrum disappeared and the PL intensity increased slightly, but FWHM parameters did not recover. On the third day, one day after the light irradiation, the peak of the PL band of the additionally exposed QDs in FDW looked like it did not undergo any spectral changes in the band position, compared to its value of the initial day (Fig. 3.6.2 a, curve 1 and 3 *), but actually during irradiation the PL band at first shifted to the short-wave side of the spectrum and then returned to its initial position during the rest of day.
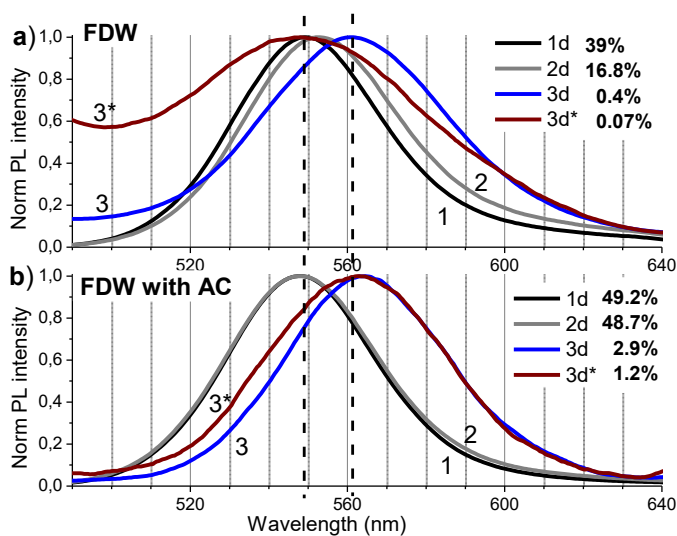

Fig. 3.6.2. The normalised PL spectral bands of CdTe-MSA quantum dots (25 mg/ml) recorded at the first, the second, and the third day as well as those of additionally exposed samples at the third day in FDW solution without (a) and with algae cells (b). $\lambda_{ex} = 405$ nm. Symbol* marks the

spectra of additionally exposed samples. The percent values were calculated
with respect to the initial PL intensity values of QDs in DW.

At the same time, the PL intensity decreased and the width at
half maximum increased even more than in the control samples (Fig.
3.6.2 a, curves 3 and 3*). In addition, the PL band of unexposed QDs
shifted even further to the long-wave side of the spectrum during the
second day, its intensity also decreased significantly and the band
broadened (Fig. 3.6.2 a, curve 3). The spectral broadening of the PL
band of CdTe-MSA quantum dots of such extent taking place after
irradiation and the shift of the PL band to the long-wave side of the
spectrum occurring after 3 hours, accompanied by an increase in PL
intensity, have not been observed yet during the spectroscopic
measurements presented in this thesis. It looks like another, fourth
stage of photomodification has been reached, which may be related
to the starting photodegradation of the QDs core, which partially
restored in the dark. However, in FDW solution with algae cells, a
decrease of the PL intensity of QDs (from 48.7% to 15.6%) as well
as a spectral shift of the PL band to long-wave side in about 6 nm
were observed after long-term irradiation, and the same spectral shift
were recorded on the third day (Fig. 3.6.2 b, curve 3). Despite the
fact that the PL intensity was lower in the exposed samples than in
the non-irradiated ones (1.2% and 2.9%, respectively), the only
difference between the normalized spectra was the irradiation-
induced broadening of the band in the short-wave part of the
spectrum (Fig. 3.6.2 b, curves 3 and 3*).

Thus, the presence of unicellular algae positively affected the
stability of the PL spectral properties of QDs in FDW. The initial
decrease of PL intensity was accompanied by a small spectral shift of
the band (Fig. 3.6.1) and a small "tail" on the long-wave part of the
PL band (Fig. 3.6.1 b), demonstrating a protective effect of QDs
compared to control samples without AC. Subsequent spectral
changes of the PL band of QDs were similar to those observed in

FDW without algae cells, including the increase of the red "tail" in the PL band (Fig. 3.6.1 b), but less pronounced (Fig. 3.6.1). The PL intensity of QDs was higher in the samples with algae cells on the third day too, and the PL band was narrower compared to the samples without algae (Fig. 3.6.2). The light-induced changes in the PL spectral properties during the experiment also depended on the presence of unicellular algae in the medium. The protective effect of AC may be related to the stabilization of the QDs capping layer. Thus, the recorded spectral changes (a smaller drop in PL intensity, a shorter spectral shift of the PL band to long-wave side and a narrower PL band with a smaller red "tail" (Figs. 3.6.1 and 3.6.2)) may together reflect a reduced ability of ions to interact with NPs in ionic media with algae due to competitive interaction with AC or their extracellular products. Therefore, algae cells can slow down the time-related, medium-induced and stimulated by irradiation decrease of the PL intensity, protecting the QDs capping layer and maintaining the irradiated QDs at an earlier stage of photomodification.

3.7. The effect of CdTe-MSA quantum dots on freshwater unicellular algae

The stabilizing effect of algae cells on the spectral properties of quantum dots can be enhanced by direct contact with QDs, where nanoparticles adhere to algae cells through non-specific interactions on the porous cell wall of the algae, or via carboxyl (-COOH) or amine ($-NH_2$) groups of the thiol ligands [35]. On the other hand, the potential adsorption of QDs on the cell surface can induce the intense responses of algae cell autofluorescence (AF). The autofluorescence spectrum measured in samples of green algae cells is mainly determined by the chlorophyll (Chls) fluorescence (FL), which has a relatively intense spectral band at 683 nm with a slope at about 740 nm. Autofluorescence of algae samples kept under periodic artificial illumination (a group I) was recorded before treatment with quantum

dots (on the first day) and measurements were continued after 24 h incubation (on the second day). The excitation wavelength at 405 nm was chosen for algae samples from the group I because of its suitability to measure quantum dots, whereas the excitation wavelength at 480 nm is the most efficient for excitation of algae autofluorescence (Fig. 3.7.1).
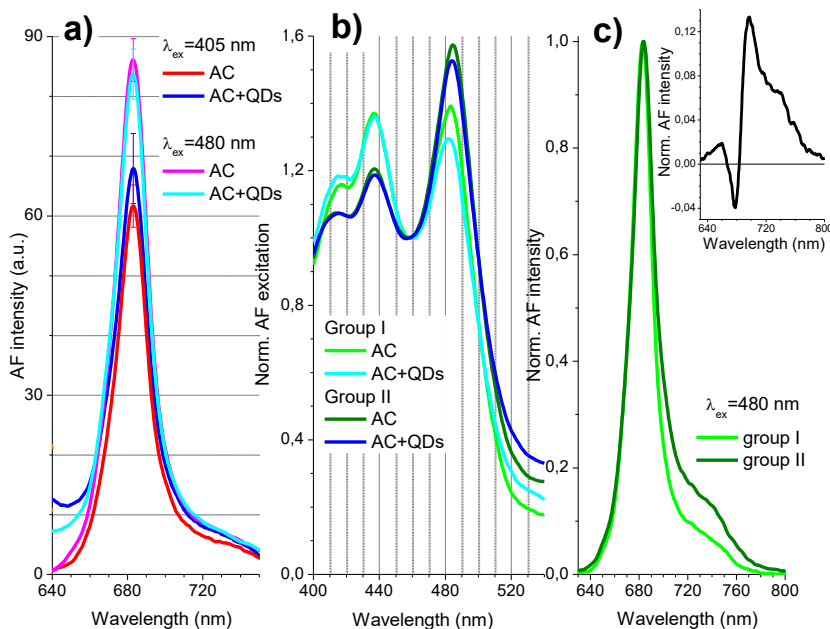
Fig. 3.7.1. (a) The autofluorescence spectra of algae being measured in control microalgae samples from the group I and those with QDs after one hour incubation; excitation wavelengths were 405 nm and 480 nm. (b) Normalised FL excitation spectra of the control algae samples and the algae samples with QDs (25 μg/ml and 100 μg/ml – in the groups I and II, respectively) being measured at a peak of the AF band of algae (about 683 nm) after 24 h incubation. (c) The autofluorescence spectra of algae samples without QDs. $\lambda_{ex} = 480$ nm. The inset shows the differential spectrum between autofluorescence of algae in the group II and in the group I.

Group I – samples kept for 12/12 hours under day/night cycle illumination conditions, group II – kept under natural daylight, avoiding direct sunlight.

Since the excitation at 405 nm is more effective for excitation of QDs than that at 480 nm, the PL of QDs contributed to the recorded fluorescence spectra of Chls, mostly at a blue spectral side. Therefore, because of an overlap of the PL band of QDs and the FL band of chlorophylls, the peak FL intensity being excited at 405 nm was higher in the spectra of algae cells with QDs than in those without QDs. An increased FL intensity of chlorophylls was expectedly registered in the spectra of all samples under excitation at 480 nm, furthermore, the FL intensity of Chls was found to be lower in the spectra of AC samples containing QDs. The FL excitation spectra of algae samples from the groups I (kept for 12/12 hours under day/night cycle illumination conditions) and II (kept under natural daylight, avoiding direct sunlight), which were registered at the peak of the FL band (683 nm) of Chls and then were normalised to a dip (at about 460 nm), are shown in figure 3.7.1 b.

The different illumination conditions of the samples in the groups I and II visibly affected the relative intensity of the peaks at about 435 nm and 485 nm, the latter being relatively enhanced in the FL excitation spectra of the control samples from the group II. The differences were also seen in the normalised fluorescence spectra (Fig. 3.7.1 c), in which the intensity of the shoulder at the red spectral region was relatively enhanced in the case of the group II as well. In both groups, however, the peak intensity was relatively lower at about 485 nm in the FL excitation spectra of algae samples with QDs as compared to that of the samples without NPs.

Thus, the altered illumination conditions of the group II samples also had an apparent effect on the normalised AF spectra of the microalgae (Fig. 3.7.1, b and c), in which the intensity of the shoulder at the red spectral region had become relatively enhanced.

Similar differences in the pattern of AF spectra might originate from spectral heterogeneity and reflect the different relative contribution of the photosystem I (PSI) and PSII, which depends on light conditions during plant growth and can vary as an adaptive response to changes in irradiance [36, 37]. Also, the size of the PSII antenna can be extensively regulated in accordance with illumination conditions [36] leading to the higher values of the Chls fluorescence measured in shaded leaves [38, 39] or considerably higher amounts of the Chls in the light harvesting centre II [40, 41]. The AF changes between microalgae from groups II and I that are seen in the differential spectrum (Fig. 3.7.1 c, an inset) also resemble a differential FL spectrum being detected in microalgae samples under conditions, in which the reaction centres of PSII are either open or closed [42]. Assuming that the algae cells in the group I were maintained at stronger illumination, there were more reaction centres of PSII in a closed state, while the group II was kept under weaker illumination, which favoured the reaction centres to be in an open state. It is likely that the observed variations in the intensity and shape of the AF spectra of two groups (Figs. 3.7.1 b and 3.7.1 c) are reflecting different photoadaptation states of microalgae.

Despite a notable effect that the adaptation of the algae samples to illumination conditions had on the relative spectral contribution of Chls to the AF intensity, as it can be seen by comparing between excitation peaks at 435 nm and at 485 nm (Fig. 3.7.1 b), the response to the presence of CdTe-MSA QDs during the first day was similar in both groups I and II: a decrease of the FL excitation peak at about 485 nm. The effect of QDs on the AF of algae cells was followed in a group I over a prolonged incubation period of 18 days, without changing the medium with QDs (Fig. 3.7.2). The statistically significant difference ($p < 0.05$) between values of the FL peak intensity of Chls (recorded from the bottom of the plates), which were evaluated using the Mann-Whitney U test, was found starting from the second day of experiment (after 24 hours of incubation).

The FL intensity in the control samples was gradually increasing in the following days, but decreasing in the samples of microalgae with QDs, and at day 18th the peak AF intensity in these samples was found to be about 4.5 times lower than in the control samples (Fig. 3.7.2). It should be noted that the increase of AF intensity in control algae samples is not due to changes in the photosynthesis apparatus of algae cell, but because of an increase in autofluorescent cells. Dose-dependent inhibition of algae growth rate that was concomitant with an enhanced production of reactive oxygen species (ROS) as well as an increase in enzymatic defence activities was observed after application of CdSe QDs [43]. The adhesion of metal oxide NPs to algae cells was shown to induce physical disruption of the cell membranes [44].
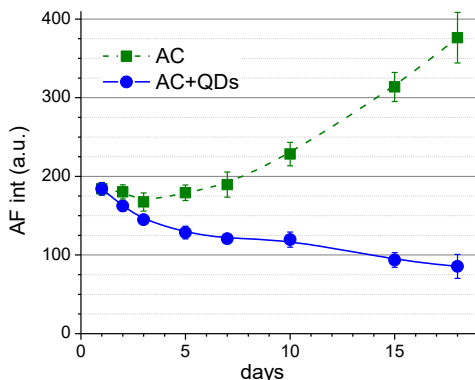
Fig. 3.7.2. The time-related variation in the averaged peak autofluorescence intensity of algae in the control samples and the samples with QDs (25 μg/ml) from the group I. $\lambda_{ex} = 405$ nm. Day 2 indicates incubation with QDs for 24 h. N = 15 in each set, a range marks 95% confidence intervals.

The microalgae samples of a group II were incubated with QDs at higher concentration (100 μg/ml) and kept under ambient daylight to diminish the photoinduced effects in NPs. The changes of AF intensity and those registered in spectral pattern are highlighted in

the differential spectra, which were obtained by normalizing two corresponding AF spectra of microalgae at one of two selected wavelengths (670 nm or 720 nm) and calculating the difference (Fig. 3.7.3).
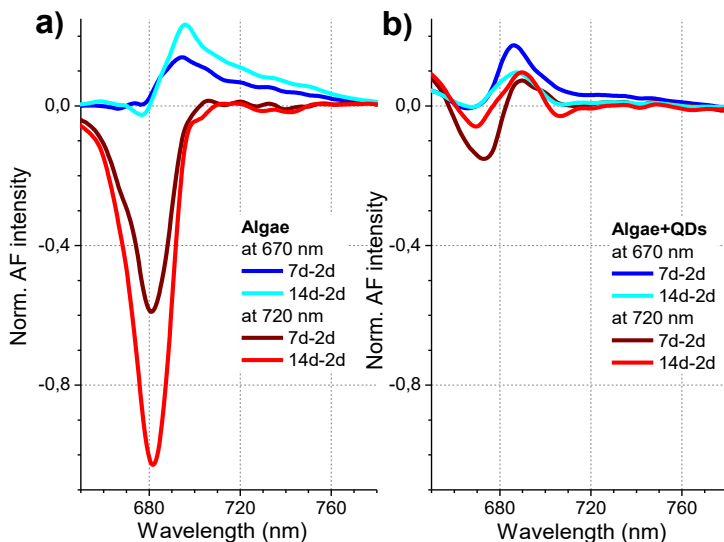
Fig. 3.7.3. The differential AF spectra of algae that show relative spectral differences between autofluorescence changes being observed with time in the control samples of algae cells and in those with QDs (100 μg/ml) from the group II; the spectra were normalised at wavelengths corresponding to a blue side (a) and a red side of the AF band (b). $\lambda_{ex} = 480$ nm. Samples were incubated with QDs starting at the 1 day.

The broad band with a sloping peak and a tail at a red side was observed in the differential spectrum after normalisation at 670 nm, which demonstrated the changes that occurred in control microalgae samples during a week (Fig. 3.7.3 a). After two weeks the relative FL intensity decreased on a blue side at about 670-690 nm, while it became even higher at above 690 nm. The differential spectra of microalgae samples being normalised at 720 nm, however, indicated just the reduction of a broad band with a dip at 683 nm, which

progressed during two weeks. The spectral changes of algae AF that were observed after two weeks incubation with QDs, however, opposed to those in control samples (Fig. 3.7.3 b). Moreover, the obtained differential pattern did not differ much regardless of the wavelength used to normalize the spectra. Thus, the progressive relative changes in two spectral regions were distinguished in the control samples kept under natural ambient light during two weeks. The spectral changes in the samples with QDs showed an opposite tendency and became more alike over time regardless of the applied normalization (Fig. 3.7.3).

The pictures of *Scenedesmus sp*. and *Chlorella sp*. algae cells, which were taken in the fluorescence mode by means of a fluorescence microscope equipped with a colour camera under excitation at UV (330-380 nm), violet (380-420 nm) and green (510-560 nm) spectral ranges as well as in the phase contrast mode, are shown in figure 3.7.4.
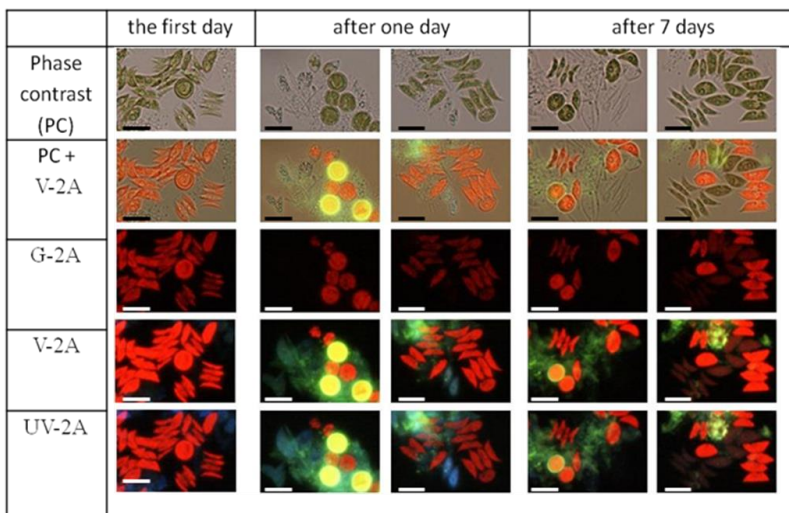

Fig. 3.7.4. The phase contrast and fluorescence images of algae cells from the samples of the group II before incubation with QDs and after incubation for 1 and 7 days. The concentration of QDs was 100 µg/ml. V-

2A excitation / emission cube with excitation range $\Delta\lambda_{ex} = 380\text{-}420$ nm, G-2A – $\Delta\lambda_{ex}=510\text{-}560$ nm and UV-2A – $\Delta\lambda_{ex} = 380\text{-}420$ nm. A scale bar is 10 μm.

The green algae cells looked red under all three excitations in a fluorescence mode of real colours, and some of algae, which looked transparent and without chlorophylls in a phase contrast mode, had a blue-coloured fluorescence, when excited at UV or violet spectral ranges. The QDs photoluminesced only under excitation at UV and violet ranges and were seen as bigger or smaller green spots. Although there were no obvious changes seen in AC using a phase contrast mode after 24 hours incubation with QDs, fluorescence images taken using UV or violet spectral excitation showed some of round-shaped *Chlorella sp.* algae starting to photoluminesce in yellow. There were also spots of green photoluminescence overlapping with the blue-fluorescing *Scenedesmus sp.* algae in samples with QDs. After the week the samples with QDs still had yellow-photoluminescing *Chlorella sp.* algae cells, but the intensity was weaker. Some clusters formed by yellow-photoluminescing quantum dots were also seen. In addition, the red fluorescence in some of apparently green *Scenedesmus sp.* algae cells was decreased in intensity as compared with the neighbouring cells or those in the samples of microalgae kept without QDs.

The influence of heavy metals cannot be ruled out in the case of the prolonged incubation of samples from the group I (Fig. 3.7.2). However, even after one week of incubation, the luminescent QDs were still observed in samples of the group II, and the microscopy imaging of incubated samples revealed no changes in cell density implying absence of direct inactivation. There was no obvious reduction in content of green chlorophylls too, observing in a phase contrast mode, but there were differences in QDs luminescence pattern as well as in the effect on AF for two algae species seen in a fluorescence mode. Some cells of *Chlorella sp.* were found to be

64

surrounded by yellow luminescence starting from the second day, which was also the case after a week, only the signal was dimmer (Fig. 3.7.4). However, no reduction in AF of *Chlorella sp*. algae has been detected. The fluorescent membranes, capable to enveloping one or even several cells, manifested in the green channel (500-590 nm), in which also PL of QDs should be detected , so it is likely that QDs accumulated specifically in this membrane and did not enter the cells (Fig. 3.7.5).
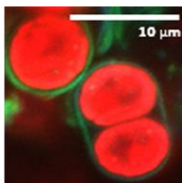
Fig. 3.7.5. The fluorescence images of algae cells from the samples of the group II after one day incubation with QDs registered with fluorescence microscope with a confocal scaning system. The concentration of QDs was 100 μg/ml. The fluorescence was excited with a diode laser λ_{ex} = 405 nm.

The notable observation concerning the fate of intracellular QDs was made in [45], reporting the rapid elimination of the PL signal due to surface modification inside the vacuoles, however, shapeless clustered photoluminescing structures were still present in the vicinity of some *Scenedesmus sp*. algae, while the red fluorescence of some cells was visibly reduced in intensity (Fig. 3.7.4). Such observation coincides with the studies demonstrating that adsorption efficacy and possible internalization of nanoparticles strongly depend on the properties of the biological systems, such as the cell type and the structure of its membrane, differentiation stage and the intercellular processes [46, 47]. Since the cellular wall serves as a selective layer protecting the algae from internalization of the nanoparticles [48, 49], as well as metal ions [50], different sensitivity of various marine microalgae to QDs, such as stronger suppression of the growth rate in the case of faster dividing species, has been

ascribed to the process of cell division itself, which makes it possible for QDs to access cellular membrane [51].

The AF peak intensity of algae samples became significantly lower in medium with CdTe-MSA quantum dots from the second day of incubation (compared to controls) and, in contrast to controls, continued to decrease during the time of experiment (18 days) (Fig. 3.7.2). A decrease in the AF intensity of some algae cells in samples with QDs was also observed in microscopy images. However, after changing the irradiation conditions, two spectral regions with different pattern of changes that were detected during the two weeks in control samples, became similar in the samples with QDs, regardless of the choice of wavelength used to normalize the spectra (Fig. 3.7.3). Therefore, it can be argued that changes being detected in unicellular algae samples without QDs reflect the adaptation response of algae photosystems to changing natural illumination. The spectral changes of algae AF measured by spectroscopic and microscopic methods in the samples with QDs thus revealed the weaker adaptive response of algae cells. In addition, although no decrease of the AF intensity of *Chlorella sp.* algae was observed, some algae cells of this species had yellow luminescent membranes surrounding one or even several cells that were likely to accumulate QDs (Fig. 3.7.5). Since membranes around several cells are formed only during the corresponding life period of *Chlorella sp*. algae (during division, and sometimes under adverse environmental conditions), it evidenced that the interaction of QDs with unicellular algae depends on the type and the physiological state of the affected cells.

4. CONCLUSIONS

1) The effect of ionic medium on the spectral properties of CdTe quantum dots capped with mercaptosuccinic acid (MSA) is reflected by a relative decrease in intensity of an excitonic absorption band

and photoluminescence of QDs, a shift in the PL band to the long-wave side of the spectrum, and a „tail" formation in the red part of the PL band. These changes reflect the interactions between ions and the QDs surface, which impair the protective effect of the capping layer of the ligands and tend to accelerate during irradiation.

2) In aqueous media the dose-dependent photomodification of CdTe-MSA quantum dots occurs in several stages, which can be determined spectroscopically by investigating various characteristics: the shape of absorption and photoluminescence spectra, the PL intensity variations during irradiation and in the dark between exposures, as well as the PL lifetime of excited states. The decrease in the quantum yield of QDs photoluminescence during the first stage depends on the initial quality of the capping layer on QDs surface. The duration of the second stage depends on ions in the medium and the ratio of them to the concentration of nanoparticles: when it increases, the stage becomes shorter. The changes in spectral characteristics observed in the third stage are characterized by accelerated aggregation of nanoparticles, which could be stimulated by the degradation of the capping ligand layer of QDs.

3) Serum albumin and the light are independent factors that can influence the spectral properties of quantum dots of varying composition in the ionic medium depending on the integral stability and the type of the surface ligand layer.

4) Serum albumin is capable to retard the ion-induced and irradiation-accelerated processes that adversely affect the surface integrity of quantum dots, as reflected by their photoluminescence spectral properties in both phosphate buffer and model ionic solutions.

5) The ion-induced and irradiation-accelerated decrease in CdTe-MSA photoluminescence intensity slows down in environment of unicellular freshwater algae, in which quantum dots are retained at an earlier stage of photomodification with reduced ability of ions from medium to interact with QDs due to their interaction with algae cells or extracellular products.

6) The effect of hydrophilic CdTe-MSA quantum dots on autofluorescence of unicellular algae occuring in the first few weeks of incubation was established by spectroscopic and microscopic methods and demonstrated dependence on the type and state of the affected cells: in the case of *Scenedesmus sp*. algae, the QDs reduced autofluorescence of algae and suppressed characteristic changes in the shape of the AF spectrum, causing a negative effect on the cellular response of photoadaptation, whereas in the case of *Chlorella sp*. algae, QDs had no significant effect on autofluorescence and accumulated on membrane, which forms only during a certain period of cellular life and can cover one or more cells.

5. SANTRAUKA (Summary in Lithuanian)

Sparti nanotechnologijų plėtra paskatino daugybės naujų medžiagų ir produktų, pasižyminčių naujomis ir neįprastomis savybėmis, atsiradimą. Fotoliuminescuojančios puslaidininkinės nanodalelės (ND) – kvantiniai taškai (KT), – naudojamos optiniuose prietaisuose arba detekcijos metoduose, kurių taikymo metu šios ND gali būti lengvai aptinkamos ir sekamos. Kvantiniai taškai pasižymi didesniu fotoliuminescencijos kvantiniu našumu ir ilgesne sužadintos būsenos gyvavimo trukme, nei šiuo metu medicinoje naudojami nestabilūs organiniai fluoroforai, ir gali, dėl paviršiaus modifikacijų, susikaupti norimoje organizmo vietoje. Todėl fotoliuminescuojantys hidrofiliniai kvantiniai taškai vis plačiau taikomi biologinių sistemų

vaizdinimui ir kaip modeliniai objektai viduląstelinių vyksmų tyrimuose. Neigiamą krūvį vandeninėse terpėse įgaunantys KT dažniausiai dengiami tiolio rūgštimis, pavyzdžiui, tioglikolio (TGR), merkaptopropionine (MPR) ir merkaptosukcinine (MSR), kurios dėl skirtingos molekulinės struktūros sudaro skirtingo stabilumo konfiguracijas su Cd molekulėmis. MSR molekulės struktūra išsiskiria tuo, kad apima tiek TGR, tiek MPR savybes, todėl gali jungtis prie vieno (kaip MPR) arba dviejų (kaip TGR) kadmio jonų.

Kadangi hidrofiliniai kvantiniai taškai skirti naudoti biologinėse aplinkose, kuriose yra jų optines savybes veikiančių ištirpusių jonų ir įvairių baltymų, šiame darbe tirtas hidrofilinių CdTe kvantinių taškų, dengtų tioliniais ligandais, optinių savybių stabilumas ir fotostabilumas skirtingose joninėse terpėse ir terpėse su serumo albuminu. Atlikti švitintų KT bandinių spektrinių savybių matavimai skirtingose vandeninėse terpėse pademonstravo, kad joninė terpės sudėtis reikšmingai paveikia šviesos sukeltus pokyčius KT spektruose, nesvarbu ar šie pokyčiai buvo sukelti tik šviesos, ar buvo kompleksiniai ir pasireiškė kartu su terpės poveikiu laike. Taigi, terpėje esantys jonai priartėdami prie KT branduolio ir adsorbuodamiesi prie jo paviršiaus sukelia „uodegos" ilgabangėje FL juostos dalyje augimą, o tada terpės jonų paskatintas ligandų atsikabinimas, sukuria sąlygas KT agregacijai, KT FL juostai paslenkant į ilgabangę pusę. Tačiau, kuris spektrinis pokytis pasireikš labiau, ir kaip intensyviai, gali priklausyti nuo jonų koncentracijos ir tipo. Švitinimas, suaktyvinantis nanodalelės paviršių, sukuria sąlygas visoms prie KT paviršiaus esančioms molekulėms persiskirstyti, ir nuo terpės sudėties priklausys, kokiu mastu po šio persiskirstymo atsidengs KT paviršiniai defektai, bei ar jie bus pasyvuojami bandinius laikant tamsoje.

Remiantis įvairiais spektroskopiniais parametrais buvo nustatytos trys universalios nuo švitinimo dozės priklausančios CdTe-MSR kvantinių taškų fotomodifikacijos stadijos pasireiškiančios ir distiliuotame vandenyje, ir terpėje su jonais, atsispindinčios tuose

69

pačiuose spektroskopiniuose parametruose: charakteringoje FL intensyvumo mažėjimo kreivėje ir smailės intensyvumo svyravimuose tamsoje tarp švitinimų, sugerties ir fotoliuminescencijos spektro formos pokyčiuose. Pirmoji stadija pasireiškė po mažiausių švitinimo dozių, ir jai buvo būdingas tik staigus FL intensyvumo kritimas, sąlygotas kvantinio našumo sumažėjimo. Tikėtina, kad pradinis švitinimas sukėlė ligandų persiskirstymą ant nanokristalo paviršiaus ir dalinį kai kurių koordinacinių ryšių nutrūkimą, todėl pirmoji stadija priklausė nuo KT dydžio ir pradinio dengiamojo sluoksnio vientisumo, o terpėje esantys jonai jai įtakos beveik neturėjo. Tačiau antroji stadija prasideda, kai nutrūksta dalis ligandus laikančių koordinacinių ryšių, ir terpės molekulės priartėja prie KT paviršiaus, todėl ši stadija akivaizdžiai priklausė nuo terpėje esančių jonų ir sutrumpėjo bandiniuose, mažėjant KT ir jonų santykiui. Trečioji fotomodifikacijos stadija pasireiškia didžiausiais ir negrįžtamais optinių savybių pokyčiais. Jos metu FL intensyvumo mažėjimo sparta vėl pagreitėjo ir net tamsoje nebeatsistatinėjo, o toliau mažėjo, sugerties spektre beveik visiškai pradingo eksitoninė juosta ties 520 nm, sumažėjo KT sužadinimo būsenos gyvavimo trukmė, o FL intensyvumui nukritus iki minimalių verčių, jos juosta pasislinko į ilgabangę spektro pusę. Kada įvyks visiškas kai kurių ligandų, pvz., MSR molekulių atkibimas, paskatinantis kvantinių taškų agregaciją, vykstančią trečiojoje stadijoje, taip pat priklauso nuo terpės jonų aktyvumo ir koncentracijos, o ne tik tiesiogiai nuo sugertos švitinimo dozės.

Eksperimentiniai rezultatai atskleidė, kad tokių pačių ir tokios pat koncentracijos kvantinių taškų spektrinių savybių stabilumas skirtingose joninėse terpėse buvo skirtingas, todėl nėra netikėta tai, kad ir albuminas darė skirtingą poveikį KT spektrinėms savybėms. Fosfatiniame buferiniame tirpale, kuriame KT FL intensyvumas iš karto po bandinių paruošimo sparčiai mažėjo, baltymas šiek tiek sulėtino šį procesą. Tačiau modelinėje joninėje terpėje, kurioje KT

FL intensyvumas buvo stabilesnis, bandiniuose su baltymu iki švitinimo FL intensyvumas staigiai sumažėjo, bet vėliau kritimas stabilizavosi. Šie skirtumai pademonstravo skirtingą baltymo poveikį ligandų ir įvairių jonų sąveikoms, vykstančioms KT paviršiuje. Kadangi fosfatinis buferinis tirpalas veikia KT spektrines savybes intensyviau nei modelinė joninė terpė, todėl ir baltymas mažiau efektyviai jas apsaugo nuo FBT esančių jonų poveikio KT paviršiaus vientisumui. Vis dėlto, BSA sumažina KT fotoliuminescencijos juostos poslinkį į ilgabangę pusę, galimai apsaugodamas nuo jonų paskatintų nanodalelių paviršiaus pažaidų ir neleisdamas jonams paspartinti fotomodifikacinius procesus švitinimo metu. Taigi, nors baltymo sąveikos pobūdis su CdTe-MSR kvantiniais taškais priklauso nuo joninėje terpėje esančių jonų, serumo albuminas geba slopinti švitinimo paskatintus jonų sukeltus procesus, neigiamai veikiančius ND paviršiaus vientisumą ir kvantinių taškų spektrines savybes tiek fosfatiniame buferiniame tirpale, tiek modelinėje joninėje terpėje.

Vandeninėje terpėje su serumo albuminu taip pat vertinta, kokią įtaką kvantinių taškų su ZnS apvalkalu spektrinių savybių fotostabilumui daro skirtingi tioliniai ligandai (TGR ir MPR). Baltymo sąveika su KT paviršiumi gali būti daugialypė, o sąveikos pobūdis priklauso ir nuo ligandų grandinėlės ilgio. Serumo albuminas negali tinkamai prisijungti prie KT padengtų MPR, nes tam trukdo ilgesnė MPR molekulės grandinėlė, tad ilgalaikis apsauginis baltyminis KT dangalas nesusiformuoja. Be to, dėl švitinimo metu pasyvuojamo kvantinio taško paviršiaus, CdSe/ZnS kvantinių taškų dengtų tiek TGR, tiek MPR ligandais FL intensyvumas po švitinimo padidėjo, ir juosta pasislinko į trumpabangę spektro pusę. Tačiau, baltymas ir šviesa yra du nepriklausomi faktoriai, veikiantys kvantinio taško paviršių, ir jų bendras poveikis gali pagerinti arba pabloginti KT optines savybes, priklausomai nuo dengiamojo paviršiaus sluoksnio sandaros ir kokybės. CdSe/ZnS kvantinių taškų, dengtų tioglikolio rūgštimi,

kvantinis našumas terpėje su serumo albuminu padidėjo, o spektrinės savybės buvo stabilesnės nei terpėje be baltymo. Taip pat švitinimas padidino CdSe/ZnS-TGR kvantinių taškų fotoliuminescencijos intensyvumą ir kvantinį našumą. Tačiau CdSe/ZnS-MPR kvantinių taškų bandinių PL intensyvumas, KN ir šių savybių stabilumas terpėje su BSA sumažėjo, o švitinimas sukėlė trumpalaikį FL intensyvumo padidėjimą.

Laukinių vienaląsčių gėlavandenių *Scenedesmus sp*. ir *Chlorella sp*. dumblių atsiradimas teigiamai paveikė CdTe dengtų MSR kvantinių taškų FL spektrinių savybių stabilumą modelinėje joninėje terpėje. Pradinis intensyvumo sumažėjimas pasireiškė kartu su mažu spektriniu smailės poslinkiu ir nedidele „uodega" ilgabangėje FL juostos pusėje, demonstruodamas apsauginį poveikį kontrolinių bandinių be dumblių atžvilgiu. Eksperimento metu šviesos sukelti FL spektrinių savybių pokyčiai taip pat priklausė nuo vienaląsčių dumblių buvimo terpėje. Registruoti spektriniai pokyčiai (mažiau kritęs FL intensyvumas, mažesnis FL juostos poslinkis į ilgabangę pusę ir siauresnė FL juosta su mažesne „uodega") drauge gali atspindėti sumažėjusią galimybę jonams, sąveikauti su ND modelinėje joninėje terpėje su dumbliais, dėl jų konkurencinės sąveikos su dumblių ląstelėmis ar jų ekstraląsteliniais produktais. Todėl dumblių ląstelės gali sulėtinti laikinį terpės sukeltą bei švitinimo paskatintą FL intensyvumo mažėjimą, apsaugodamos KT dengiamąjį sluoksnį ir išlaikydamos švitintus KT ankstyvesnėje fotomodifikacijos stadijoje.

Įvertinus KT fotostabilumą terpėje su dumblių ląstelėmis, spektroskopiniais ir mikroskopiniais metodais ištirti kvantinių taškų sukelti dumblių autofluorescencijos pokyčiai bei stebėtas nanodalelių poveikis dumblių fotoadaptaciniam atsakui. Mikroskopu gautuose vaizduose taip pat buvo stebimas kai kurių *Scenedesmus sp*. dumblių AF intensyvumo sumažėjimas bandiniuose su KT. Pasikeitus švitinimo sąlygoms, per dvi savaites stebimuose kontroliniuose bandiniuose išskirtos dvi spektrinės sritys su skirtingais pokyčiais,

bandiniuose su KT supanašėjo, nepriklausomai nuo pasirinktos normavimo srities. Todėl, galima teigti, kad pokyčiai dumblių bandiniuose be KT atspindi dumblių fotosistemų prisitaikymo prie besikeičiančio natūralaus apšvietimo atsaką. Išmatuoti dumblių spektriniai pokyčiai bandiniuose su KT atskleidžia, kad buvo užregistruotas silpnesnis dumblių ląstelių adaptacinis atsakas. Be to, nors jokio *Chlorella* sp. dumblių AF intensyvumo sumažėjimo nebuvo aptikta, dalis šios rūšies dumblių ląstelių turėjo geltonai liuminescuojančias membranas, apgaubiančias vieną arba net kelias ląsteles, kuriose, tikėtina, galėjo susikaupti kvantiniai taškai. Kadangi membranos aplink kelias ląsteles susidaro tik atitinkamu *Chlorella* sp. dumblių gyvavimo laikotarpiu (dalijimosi metu, o kartais ir nepalankiomis aplinkos sąlygomis), panašu, kad KT sąveika su vienaląsčiais dumbliais priklauso nuo paveiktų ląstelių rūšies ir būsenos.

Darbo tikslas ir uždaviniai

Darbo tikslas
Ištirti hidrofilinių kvantinių taškų (KT) fotostabilumą modelinėse biosistemose skirtingomis aplinkos sąlygomis ir šių nanodalelių fototoksinį poveikį vienaląsčiams gėlavandeniams dumbliams.

Darbo uždaviniai:
1) Ištirti šviesos poveikį CdTe kvantinių taškų dengtų merkaptosukcinine rūgštimi (MSR) spektrinėms savybėms ir įvertinti jų pokyčių priklausomybę nuo švitinimo dozės.

2) Įvertinti joninės terpės ir serumo albumino poveikį tioliais dengtų CdTe ir CdSe/ZnS kvantinių taškų optinių savybių stabilumui ir fotostabilumui.

3) Palyginti tioglikolio ir merkaptopropionine rūgšties ligandų įtaką CdSe/ZnS kvantinių taškų spektrinių savybių stabilumui ir fotostabilumui vandeninėje buferinėje terpėje su serumo albuminu.

4) Ištirti vienaląsčių žaliųjų gėlavandenių *Scenedesmus sp.* dumblių poveikį hidrofilinių CdTe-MSR kvantinių taškų spektrinių savybių stabilumui ir fotostabilumui modelinėje joninėje terpėje.

5) Spektroskopiniais ir mikroskopiniais metodais ištirti hidrofilinių CdTe-MSR kvantinių taškų sukeltus vienaląsčių *Scenedesmus sp.* dumblių autofluorescencijos pokyčius ir įvertinti KT poveikį dumblių fotoadaptaciniam atsakui.

MOKSLINIS NAUJUMAS IR AKTUALUMAS

Šiame darbe pirmą kartą nustatytos nuo švitinimo dozės priklausančios kelios kvantinių taškų fotomodifikacijos stadijos, kurios atsispindėjo įvairiuose spektroskopiniuose parametruose: FL intensyvumo mažėjimo kreivėje ir intensyvumo atsistatinėjimo tamsoje dėsningumuose, sugerties ir fotoliuminescencijos spektro formos pokyčiuose bei FL gyvavimo trukmių kinetikose. Šios fotomodifikacijos stadijos apjungtos į bendrą šviesos poveikio kvantiniams taškams vandeninėje terpėje schemą.

Pirmą kartą parodyta, kaip KT optinių savybių stabilumo priklausomybę nuo švitinimo dozės paveikia joninė terpė. Parodyta, kaip nuo ardančio švitinimo poveikio apsaugo serumo albuminas ir vienaląsčiai dumbliai. Pademonstruota, kad šie išoriniai veiksniai pirmiausia veikia kvantinio taško paviršių, todėl galutinis poveikis KT stabilumui bei sukelti optinių savybių pokyčiai labiau priklauso nuo dengiamojo sluoksnio ligandų atsako, o ne nuo kvantinių taškų branduolį gaubiančio apvalkalo.

Nustatytas priklausomybės nuo švitinimo dozės pobūdis, veikiant kvantinius taškus jonais, prisideda prie galimybės kvantinius taškus panaudoti, kaip jonų biojutiklius, pavyzdžiui, vertinant vandens taršą.

Taip pat fluorescencinės mikroskopijos metodu pirmą kartą pastebėta kvantinių taškų fotoliuminescencija ant dumblių ląstelių

membranų. Aptikta kai kurių dumblių ląstelių savybė sukaupti dalį kvantinių taškų ant membranos ir nebūti pažeistoms, atvertų galimybes ateityje panaudoti dumblių ląsteles kvantinių taškų surinkimui, nanodalelėms pakliuvus į vandens telkinius.

Kadangi nanotechnologijos yra sparčiai besivystanti sritis, daugybė mokslinių tyrimų atliekama su nanomedžiagomis. Tačiau dėl nanodalelių įvairovės ir jų savybių priklausomybės nuo aplinkos sąlygų mokslinėje literatūroje yra pateikiama daugybė prieštaringos informacijos apie išorinių veiksnių įtaką kvantinių taškų savybėms. Šiame darbe pateikti rezultatai apie hidrofilinių kvantinių taškų fotostabilumą ir fototoksiškumą modelinėse biosistemose prisidės prie bendro švitinimo ir terpės poveikio optinėms nanodalelių savybėms mechanizmo aiškinimo, apibendrinant įvairių tyrimų rezultatus, ir padės ne tik efektyviau taikyti nanodaleles, bet ir apsisaugoti nuo tam tikromis sąlygomis žalingo jų poveikio

GINAMIEJI TEIGINIAI

1) CdTe kvantinių taškų, dengtų merkaptosukcinine rūgštimi (MSR), fotoliuminescencijos fotoblukimo vandeninėse terpėse priklausomybė nuo švitinimo dozės susijusi su registruojamais fotoliuminescencijos ir sugerties spektrų intensyvumų ir formos pokyčiais.

2) Serumo albumino ir šviesos poveikiai optinėms hidrofilinių kvantinių taškų savybėms priklauso nuo dengiamojo ligandų sluoksnio kokybės ir joninės terpės sudėties.

3) Vienaląsčiai dumbliai dalinai stabilizuoja CdTe-MSR kvantinių taškų spektrines savybes jų stabilumą bloginančių veiksnių aplinkoje, kurią sąlygoja terpės joninė sudėtis ir švitinimas.

4) CdTe-MSR kvantiniai taškai paveikia vienaląsčių dumblių ląstelių autofluorescencijos intensyvumą ir spektrinę formą bei daro neigiamą įtaką jų fotoadaptaciniams atsakams.

IŠVADOS

1) Joninės terpės poveikis CdTe kvantinių taškų dengtų merkaptosukcinine rūgštimi (MSR) spektrinėms savybėms pasireiškia santykiniu eksitoninės KT sugerties juostos ir fotoliuminescencijos intensyvumo sumažėjimu, FL juostos poslinkiu į ilgabangę pusę ir „uodegos" formavimusi FL spektro raudonojoje dalyje. Šie pokyčiai atspindi jonų sąveikas su KT paviršiumi, slopstant dengiamojo ligandų sluoksnio apsauginiam poveikiui, ir spartėja švitinimo metu.

2) Vandeninėse terpėse nuo švitinimo dozės priklausanti CdTe-MSR kvantinių taškų fotomodifikacija vyksta keliomis stadijomis, kurias galima nustatyti spektroskopiniais metodais tiriant įvairias charakteristikas: sugerties ir fotoliuminescencijos spektrų formą, fotoliuminescencijos intensyvumo svyravimus švitinimo metu ir tamsoje tarp poveikių bei sužadintųjų būsenų fotoliuminescencijos gyvavimo trukmę. KT fotoliuminescencijos kvantinio našumo sumažėjimas pirmosios stadijos metu priklauso nuo pradinės dengiamojo paviršiaus sluoksnio kokybės. Antrosios stadijos trukmė priklauso nuo terpėje esančių jonų bei jų ir nanodalelių koncentracijų santykio: jam didėjant, stadija trumpėja. Trečiosios stadijos metu stebimi spektrinių charakteristikų pokyčiai būdingi spartėjančiai nanodalelių agregacijai, kurią galėtų skatinti yrantis kvantinių taškų dengiamojo ligandų sluoksnis.

3) Serumo albuminas ir šviesa yra nepriklausomi veiksniai, darantys įtaką skirtingos sudėties kvantinių taškų spektrinėms savybėms,

priklausančioms nuo skirtingos sandaros kvantinių taškų paviršinio ligandų sluoksnio vientisumo pokyčių joninėje terpėje.

4) Serumo albuminas geba slopinti jonų sukeltus ir švitinimo paskatintus procesus, neigiamai veikiančius kvantinių taškų paviršiaus vientisumą, kurį atspindi jų fotoliuminescencijos spektrinės savybės ir fosfatiniame buferiniame tirpale, ir modelinėje joninėje terpėje.

5) Joninės terpės sukeltas bei švitinimo paskatintas CdTe-MSR fotoliuminescencijos intensyvumo mažėjimas sulėtėja vienaląsčių gėlavandenių dumblių aplinkoje, išlaikančioje kvantinius taškus ankstyvesnėje fotomodifikacijos stadijoje, sumažėjus galimybei terpės jonams sąveikauti su KT dėl jų abiejų sąveikos su dumblių ląstelėmis bei ekstraląsteliniais produktais.

6) Spektroskopiniais ir mikroskopiniais metodais nustatyta, kad hidrofilinių CdTe-MSR kvantinių taškų poveikis vienaląsčių dumblių autofluorescencijai pirmosiomis inkubacijos savaitėmis priklauso nuo paveiktų ląstelių rūšies ir būsenos: *Scenedesmus sp.* dumblių atveju KT sumažina jų autofluorescenciją ir slopina charakteringus AF spektro formos pokyčius, sukeldami neigiamą poveikį fotoadaptaciniam ląstelių atsakui, o *Chlorella* sp. dumblių atveju KT pastebimo poveikio autofluorescencijai nedaro ir susikaupia ant membranos, kuri suformuojama tik tam tikru ląstelių gyvavimo laikotarpiu ir apgaubia vieną ar kelias ląsteles.

LIST OF PUBLICATIONS

Publications listed in the *Thomson Reuters Web of Science* database:

1. A. Kalnaitytė, S. Bagdonas, R. Rotomskis. Effect of light on stability of thiol-capped CdSe/ZnS quantum dots in the presence of albumin. Lithuanian Journal of Physics, Vol. 54, No. 4, pp. 256–265 (2014).
2. A. Kalnaitytė, S. Bagdonas, R. Rotomskis. The dose-dependent photobleaching of CdTe quantum dots in aqueous media. Journal of Luminescence, 201 (2018) 434–44.

Presentation in national and international conferences:

1. A. Kalnaitytė, S. Bagdonas, R. Rotomskis, Effects of protein and light on stability of CdSe/Zn-TGR quantum dots in aqueous media: spectroscopic study, Open Readings 2012, kovas, Vilnius, Lietuva.
2. A. Kalnaitytė, S. Bagdonas, Puslaidininkinių kvantinių taškų fotostabilumo tyrimai vandeninėse ir biologinėse modelinėse terpėse, Studentų mokslinių tyrimų 2011-2012 metų konferencija, 2012, Vilnius, Lietuva.
3. A. Kalnaitytė, S. Bagdonas, R. Rotomskis, Spectroscopic study of quantum dots photostability in aqueous and biological model systems, 2013, 40-oji Lietuvos nacionalinė fizikos konferencija, Vilnius, Lietuva.
4. A. Kalnaitytė, S. Bagdonas, R. Rotomskis, Effects of blue light on stability and toxicity of CdSe quantum dots in media with microalgae: spectroscopic and microscopic study, 2014, Open Readings 2014, kovas, Vilnius, Lietuva.
5. A. Kalnaitytė, S. Bagdonas, R. Rotomskis, Photostability and toxicity of quantum dots in media with microalgae, Nanotechnology: Research and Development, 2014, gegužės 15-16, Vilnius, Lietuva.
6. A. Kalnaitytė, S. Bagdonas, Photostability and toxicity of CdSe hydrophilic quantum dots in media with freshwater algae, Naujametė fizikos konferencija LTφ, 2015 m. sausio 2-3 d. Vilniaus universitetas, Fizikos fakultetas.

7. A. Kalnaitytė, S. Bagdonas, CdTe kvantinių taškų ir mėlynos spinduliuotės poveikiai gėlavandeniams vienaląsčiams dumbliams, 41-oji Lietuvos nacionalinė fizikos konferencija, 2015 m. birželio 17-19 d. Vilnius.

8. A. Kalnaitytė, S. Bagdonas, R. Rotomskis, Photostability of hydrophilic quantum dots in the presence of albumin and in the medium with algae cells, 16th Congress of the European Society for Photobiology, rugpjūčio 31 d. – rugsėjo 4 d., 2015, Aveiro, Portugalija.

9. A. Kalnaitytė, S. Bagdonas, R. Rotomskis, Photostability of core and core/shell quantum dots in the presence of albumin and in mouse fibroblast cells, Open Readings 2017, kovo 14-17 d. Vilnius, Lietuva.

10. A. Kalnaitytė, S. Bagdonas, Photoinduced changes in spectral properties of CdTe quantum dots in the presence of ions and albumin, 17th Congress of the European Society for Photobiology, rugsėjo 4 – 8, 2017, Piza, Italija.

11. A. Kalnaitytė, S. Bagdonas, R. Rotomskis, Šviesos sukelti CdTe kvantinių taškų spektrinių savybių pokyčiai modelinėse ir biologinėse terpėse, 42-oji Lietuvos nacionalinė fizikos konferencija, 2017 m. spalio 4-6 d. Vilnius.

12. I. A. Jakaitytė, A. Kalnaitytė, S. Bagdonas, Effects of heavy metals ions and quantum dots on the autofluorescence of freshwater microalgae, Open Readings 2019, kovas, Vilnius, Lietuva.

13. S. Bagdonas, V. Karabanovas, V. Poderys, A. Kalnaitytė, G. Jarockytė, R. Rotomskis, Luminescent nanoparticles for cellular imaging and theranostics, Conference Photonics North 2019, gegužės 21-23 d., Kvebekas, Kanada.

Other publications and presentations:

1. A. Kalnaitytė, S. Bagdonas, Photoinduced bleaching and degradation of chlorophylls in freshwater algae, OpenReadings 2015, kovo 24-27 Vilnius, Lietuva.

REFERENCES

1. A. Hoshino, K. Fujioka, T. Oku, M. Suga, Y. F. Sasaki, T. Ohta, M. Yasuhara, K. Suzuki, K. Yamamoto, Physicochemical properties and cellular toxicity of nanocrystal quantum dots depend on their surface modification, Nano Lett, 4, (2004), 2163-9.

2. G. H. Krause, E.Weis, Chlorophyll fluorescence and photosynthesis: the basics, Annu. Rev.Plant Physiol. Plant Mol. Biol., 42, (1991), 313-49.

3. G. H. Krause, E. Weis, Chlorophyll fluorescence as a tool in plant physiology. II. Interpretation of fluorescence signals, Photosynthesis Research, 5, (1984), 139-157.

4. D. F. Eaton, Reference materials for fluorescence measurement, Pure Appl. Chem., 60(7), (1988), 1107–1114.

5. M. Daimon, A. Masumura, Measurement of the refractive index of distilled water from the near-infrared region to the ultraviolet region, Appl. Opt., 46(18), (2007), 3811–3820.

6. J. Nowakowska, The Refractive Indices of Ethyl Alcohol and Water Mixtures, Master's Theses, Paper 668, Loyola University, Chicago, 1939.

7. Y. Zhang, L. Mi, P. N. Wang, J. Ma, J. Y. Chen, pH-dependent aggregation and photoluminescence behavior of thiol-capped CdTe quantum dots in aqueous solutions, J. of Lumines., 128, (2008), 1948–1951.

8. M. V. Artemyev, U. Woggon, H. Jaschinski, L.I. Gurinovich, S.V. Gaponenko, Spectroscopic Study of Electronic States in an Ensemble of Close-Packed CdSe Nanocrystals, J. Phys. Chem. B, 104, (2000), 11617.

9. M. Noh, T. Kim, H. Lee, C. K. Kim, S. W. Joo, K. Lee, Fluorescence quenching caused by aggregation of water-soluble CdSe quantum dots, Colloids and Surfaces A: Physicochem. Eng. Aspects, 359, (2010), 39–44.

10. Y. Zhang, Y. Chen, P. Westerhoff, J. C. Crittenden, Stability and Removal of Water Soluble CdTe Quantum Dots in Water, Environ. Sci. Technol., 42, (2008), 321–325.

11. A. V. Isarov, J. Chrysochoos, Optical and photochemical properties of nonstoichiometric cadmium sulphide nanoparticles: surface modification with copper (II) ions, Langmuir, 13, (1997), 3142–3149.

12. Y. S. Xia, C. Q. Zhu, Use of surface-modified CdTe quantum dots as fluorescent probes in sensing mercury (II), Talanta, 75, (2008), 215–221.

13. S. A. Blanton, M. A. Hines, P. Guyot-Sionnest, Photoluminescence wandering in single CdSe nanocrystals, Appl. Phys. Lett., 69, (1996), 3905–3907.

14. Y.F. Liu, J.S. Yu, Selective synthesis of CdTe and high luminescence CdTe/CdS quantum dots: the effect of ligands, J. Colloid Interface Sci., 333, (2009), 690–698.

15. M. Jones, J. Nedeljkovic, R.J. Ellingson, A.J. Nozik, G. Rumbles, Photoenhancement of luminescence in colloidal CdSe quantum dot solutions, J. Phys. Chem. B, 107, (2003), 11346–11352.
16. Z. Yuan, A. Zhang, Y. Cao, J. Yang, Y. Zhu, P. Yang, Effect of mercaptocarboxylic acids on luminescent properties of CdTe quantum dots, J. Fluoresc., 22, (2012), 121–127.
17. J. Aldana, N. Lavelle, Y.J. Wang, X.G. Peng, Size dependent dissociation pH of thiolate ligands from cadmium chalcogenide nanocrystals, J. Am. Chem. Soc., 127, (2005), 2496–2504.
18. S. Emin, A. Loukanov, M. Wakasa, S. Nakabayashi, Y. Kaneko, Photostability of water-dispersible CdTe quantum dots: capping ligands and oxygen, Chem. Lett., 39, (2010), 654656.
19. A. S. Tsipotan, M. A. Gerasimova, A. S. Aleksandrovsky, S. M. Zharkov, V. V. Slabko, Effect of visible and UV irradiation on the aggregation stability of CdTe quantum dots, J. Nanopart. Res, 18, (2016), 324.
20. J. Ma, J.Y. Chen, Y. Zhang, P.N. Wang, J. Guo, W.L. Yang, C.C. Wang, Photochemical instability of thiol-capped CdTe quantum dots in aqueous solution and living cells: process and mechanism, J. Phys. Chem. B, 111, (2007), 12012.
21. J. Aldana, Y.A. Wang, X.G. Peng, Photochemical instability of CdSe nanocrystals coated by hydrophilic thiols. J. Am. Chem. Soc., 123, (2001), 8844–8850.
22. S. R. Cordero, P. J. Carson, R. A. Estabrook, G. F. Strouse, S. K. Buratto, Photo-activated luminescence of CdSe quantum dot monolayers, J. Phys. Chem. B, 104, (2000), 12137–12142.
23. K. Pechstedt, T. Whittle, J. Baumberg, T. Melvin, Photoluminescence of colloidal CdSe/ZnS quantum dots: the critical effect of water molecules, J. Phys. Chem. C, 114, (2010), 12069–12077.
24. Y. S. Xia, C. Cao, C. Q. Zhu, Two distinct photoluminescence responses of CdTe quantum dots to Ag (I), J Lumin, 128, (2008), 166-172.
25. Q. Wang, Y. Kuo, Y. Wang, G. Shin, Ch. Ruengruglikit, Q. Huang, Luminescent properties of water- soluble denatured bovine serum albumin-coated CdTe quantum dots, J. Phys. Chem. B, 110, (2006), 16860–16866.
26. V. Poderys, M. Matulionyte, A. Selskis, R. Rotomskis, Interaction of water-soluble CdTe quantum dots with bovine serum albumin, Nanoscale Res. Lett., 6, (2011), 9.
27. B. Sahoo, M. Goswami, S. Nag, S. Maiti, Spontaneous formation of a protein corona prevents the loss of quantum dot fluorescence in physiological buffers, Chem. Phys. Lett., 445, (2007), 217–220.

28. E. S. Shibu, M. Hamada, S. Nakanishi, S. Wakida, V. Biju, Photoluminescence of CdSe and CdSe/ZnS quantum dots: Modifications for making the invisible visible at ensemble and single-molecule levels, Coordination Chemistry Reviews, 263– 264, (2014), 2– 12.

29. F. Aldeek, L. Balan, J. Lamber, R. Schneider, The influence of capping thioalkyl acid on the growth and photoluminescence efficiency of CdTe and CdSe quantum dots, Nanotechnology, 19, (2008), 475401 (9).

30. A. M. Derfus, W. C. W. Chan, S. N. Bhatia, Probing the cytotoxicity of semiconductor quantum dots. Nano Lett., 4(1), (2004), 11−18.

31. E. Morelli, E. Salvadori, R. Bizzarri, P. Cioni, E. Gabellieri, Interaction of CdSe/ZnS quantum dots with the marine diatom Phaeodactylum tricornutum and the green alga Dunaliella tertiolecta: A biophysical approach, Biophysical Chemistry, 182, (2013), 4–10.

32. S. Zhang, Y. Jiang, C. Chen, J. Spurgin, K.A. Schwehr, A. Quigg,W. Chin, P.H. Santschi, Aggregation, dissolution, and stability of quantum dots in marine environments: importance of extracellular polymeric substances, Environ. Sci. Technol., 46, (2012), 8764–8772.

33. S. Zhang, Y. Jiang, C. Chen, D. Creeley, K.A. Schwehr, A. Quigg, W. Chin, P.H. Santschi, Ameliorating effects of extracellular polymeric substances excreted by Thalassiosira pseudonana onalgal toxicity of CdSe quantum dots, Aquat. Toxicol., 126, (2013), 214–223.

34. P. Chen, B. A. Powell, M. Mortimer, P. C. Ke, Adaptive Interactions between Zinc Oxide Nanoparticles and Chlorella sp., Environ. Sci. Technol. 46, (2012), 12178−12185.

35. S. Lin, P. Bhattacharya, N. C. Rajapakse, D. E. Brune, P. Chun Ke, Effects of Quantum Dots Adsorption on Algal Photosynthesis, J. Phys. Chem. C, 133, (2009), 10962–10966.

36. R. Pedros, I. Moya, Y. Goulas, S. Jacquemoud, Chlorophyll fluorescence emission spectrum inside a leaf, Photochem. Photobiol. Sci., 7, (2008), 498–502.

37. F. Franck, P. Juneau, R. Popovic, Resolution of the Photosystem I and Photosystem II contributions to chlorophyll fluorescence of intact leaves at room temperature, Biochimica et Biophysica Acta, 1556, (2002), 239–246.

38. S. Malkin, D. Fork, Photosynthetic Units of Sun and Shade Plants, Plant Physiol., 67, (1981), 580-583.

39. S. Malkin, P. A. Armond, H. A. Mooney, D. C. Fork, Photosystem II Photosynthetic Unit Sizes from Fluorescence Induction in Leaves: Correlation to photosynthetic capacity, Plant Physiol., 67, (1981), 570-579.

40. H. K. Lichtenthaler, F. Babani, Light Adaptation and Senescence of the Photosynthetic Apparatus. Changes in Pigment Composition, Chlorophyll Fluorescence Parameters and Photosynthetic Activity, Chapter 28 from George C. Papageorgiou and Govindjee (eds): Chlorophyll a Fluorescence: A Signature of Photosynthesis, 2004, 713-736.

41. H. K. Lichtenthaler, G. Kuhn, U. Prenzel, D. Meier, Chlorophyll-protein levels and degree of thylakoid stacking in radish chloroplasts from high-light, low-light and bentazon-treated plants, Physiologia Plantarum, 56-2, (1982), 183-188.

42. F. Rizzo, G. Zucchelli, R. Jennings, S. Santabarbara, Wavelength dependence of the fluorescence emission under conditions of open and closed Photosystem II reaction centres in the green alga Chlorella sorokiniana, Biochimica et Biophysica Acta, 1837, (2014), 726–733.

43. E. Morellia, P. Cionia, M. Posarelli, E. Gabellieri, Chemical stability of CdSe quantum dots in seawater and their effects on a marine microalga, Aquatic Toxicology, 122– 123, (2012), 153– 162.

44. N. B. Hartmann, F. Von der Kammer, T. Hofmann, M. Baalousha, S. Ottofuelling, A. Baun, Algal testing of titanium dioxide nanoparticles—Testing considerations, inhibitory effects and modification of cadmium bioavailability, Toxicology, 269, (2010), 190–197.

45. Y. Wang, A-J Miao, J. Luo, Z.-B Wei, J-J Zhu, L-Y Yang, Bioaccumulation of CdTe Quantum Dots in a Freshwater Alga Ochromonas danica: A Kinetics Study, Environ. Sci. Technol., 47, (2013), 10601−10610.

46. A. Oukarroum, S. Bras, F. Perreault, R. Popovic, Inhibitory effects of silver nanoparticles in two green algae, Chlorella vulgaris and Dunaliella tertiolecta, Ecotoxicology and Environmental Safety, 78, (2012), 80–85.

47. A. E. Nel, L. Mädler, D. Velegol, T. Xia, E. M. V. Hoek, P. Somasundaran, F. Klaessig, V. Castranova, M. Thompson, Understanding biophysicochemical interactions at the nano–bio interface, Nat. Mater., 8, (2009), 543–557.

48. I. A. M. Worms, J. Boltzman, M. Garcia, V. I. Slaveykova, Cell-wall-dependent effect of carboxyl-CdSe/ZnS quantum dots on lead and copper availability to green microalgae, Environ. Pollut., 167, (2012), 27–33.

49. N. von Moos, P. Bowen, V. I. Slaveykova, Bioavailability of inorganic nanoparticles to planktonic bacteria and aquatic microalgae in freshwater, Environ. Sci.: Nano, 1, (2014), 214–232.

50. S. M. Macfie, P. M. Welbourn, The Cell Wall as a Barrier to Uptake of Metal Ions in the Unicellular Green Alga Chlamydomonas reinhardtii (Chlorophyceae), Arch. Environ. Contam. Toxicol., 39, (2000), 413–419.

51. Ch. Zhou, V. Vitiello, D. Pellegrini, Ch. Wu, E. Morelli, I. Buttino, Toxicological effects of CdSe/ZnS quantum dots on marine planktonic organisms, Ecotoxicology and Environmental Safety, 123, (2016), 26–31.

CURRICULUM VITAE

NAME   **AGNĖ KALNAITYTĖ**

E-MAIL   agne.kalnaityte@ff.vu.lt, agne.kalnaityte@gmail.com

EDUCATION

1996 – 2008	**Kartena secondary school.** Secondary education.
2005– 2008	**Šiauliai University, Junior physicist's school "PHOTON".** General subjects of physics. Higher Level.
2008 – 2012	**Vilnius University. Bachelor Degree in Physics.** Study program: Modern Technologies Physics and Management. Main subjects: higher mathematics, mechanics, electrodynamics, lasers and light technologies, computer sciences, human resources management, firm economics, banking and finances.
2012 – 2014	**Vilnius University. Master's Degree in Biophysics.** Study program: Biophysics Main subjects: biophotonics, photobiology, biophysical nanotechnologies, kinetics spectroscopy, laser in biology and medicine.
2014– 2018	**Vilnius University. Doctoral (PhD) studies in Biophysics.**

WORK EXPERIENCE

2011-2012	Students' research practice in Vilnius University Department of Quantum Electronics: Spectroscopic study of quantum dots photostability in aqueous and biological model systems.
2014	Additional practice during studies financed by European Social Fund Project No. VP1-2-2-ŠMM-09-V-01-005: "The Impact of Quantum Dots' Coating on Their Photostability and Vital Cellular Processes".

2015-2018	Laboratory assistant position in Vilnius University, Biophotonics Teaching Laboratory
2016-2018	Engineer position in in Vilnius University the Interfaculty General Physics Teaching Laboratory for students from the Medicine, Natural Sciences and Chemistry Faculties.
Since 2018	Teaching assistant position in Vilnius University Laser Research Center.
Since 2019	Junior researcher position in Vilnius University Laser Research Center.

EDUCATIONAL ACTIVITY

Since 2016	Lector of „Methods of environmental pollution investigation" at Vilnius University Faculty of Physics.
Since 2018	Lector of „Introduction to the physics of living systems", „Methods of biological objects investigation" and „Laser application in biology and medicine" at Vilnius University Faculty of Physics.

NOTES

NOTES